Brain Structure and Function (2020) 225:285–304
https://doi.org/10.1007/s00429-019-01989-4

ORIGINAL ARTICLE

Electrophysiology and distribution of oxytocin and vasopressin neurons in the hypothalamic paraventricular nucleus: a study in male and female rats

Alan Kania[1,2] · Patryk Sambak[1] · Anna Gugula[1] · Agata Szlaga[1] · Zbigniew Soltys[3] · Tomasz Blasiak[1] · Grzegorz Hess[1] · Zenon Rajfur[4] · Anna Blasiak[1]

Received: 22 May 2019 / Accepted: 15 November 2019 / Published online: 9 December 2019

Abstract

Magnocellular neurosecretory cells (MNCs) clustered in the hypothalamic paraventricular nucleus (PVN) and supraoptic nucleus constitute a major source of oxytocin (OXT) and arginine vasopressin (AVP) peptides, and are among the best described peptidergic neurons in the brain. OXT and AVP are involved in a range of homeostatic processes, social behaviours, emotional processes, and learning. Notably, their actions can be sex-specific, and several sex differences in the anatomies of the OXT and AVP systems have been reported. Nonetheless, possible sex differences in the detailed distributions of MNCs and in their intrinsic electrical properties ex vivo have not been extensively examined. We addressed these issues utilizing immunostaining and patch-clamp ex vivo recordings. Here, we showed that Sprague-Dawley rat PVN AVP neurons are more numerous than OXT cells and that more neurons of both types are present in males. Furthermore, we identified several previously unreported differences between putative OXT and AVP MNC electrophysiology contributing to their partially unique profiles. Notably, elucidation of the highly specific action potential (AP) shapes, with AVP MNCs having a narrower AP and faster hyperpolarizing after-potential (HAP) kinetics than OXT MNCs, allowed unambiguous discrimination between OXT and AVP MNCs ex vivo for the first time. Moreover, the examined electrophysiological properties of male and female MNCs generally overlapped with the following exceptions: higher membrane resistance in male MNCs and HAP kinetics in putative OXT MNCs, which was slower in males. These reported observations constitute a thorough addition to the knowledge of MNC properties shaping their diverse physiological actions in both sexes.

Keywords Paraventricular nucleus of the hypothalamus · Magnocellular neurosecretory cells · Oxytocin · Vasopressin · Sex differences · Electrophysiology

Introduction

The paraventricular hypothalamic nucleus (PVN) is considered a major hub of homeostatic control in mammals. Composed of functionally distinct neuronal populations, the

Electronic supplementary material The online version of this article (https://doi.org/10.1007/s00429-019-01989-4) contains supplementary material, which is available to authorized users.

✉ Anna Blasiak
anna.blasiak@uj.edu.pl

Alan Kania
alan.kania@uj.edu.pl

[1] Department of Neurophysiology and Chronobiology, Institute of Zoology and Biomedical Research, Jagiellonian University, Gronostajowa 9, 30-387 Krakow, Poland

[2] Pharmacology Unit, School of Pharmacy, University of Camerino, Camerino, Italy

[3] Department of Neuroanatomy, Institute of Zoology and Biomedical Research, Jagiellonian University, 30-387 Krakow, Poland

[4] Faculty of Physics, Astronomy and Applied Computer Science, Institute of Physics, Jagiellonian University, 30-348 Krakow, Poland

PVN contributes to hypothalamic neurosecretory systems (magno- and parvocellular neurosecretory cells) and the central autonomic network (brain stem and spinal cord projecting parvocellular neurons). Integrating and orchestrating neuroendocrine and autonomic responses, the PVN controls a range of physiological and behavioural processes, such as stress response, energy and fluid balance, metabolism, nociception, reproduction, and social behaviours (Hazell et al. 2012; Horn and Swanson 2013; Armstrong 2015).

Magnocellular neurosecretory cells (MNCs) of the PVN, together with those clustered in the hypothalamic supraoptic nucleus (SON) and accessory nuclei, are the major source of oxytocin (OXT) and arginine vasopressin (AVP) peptides (Silverman and Zimmerman 1983; Hou-Yu et al. 1986). OXT and AVP MNCs robustly project to the neurohypophysis, where OXT and AVP are released into circulation to act peripherally as hormones in several physiological processes: OXT release is crucial for labour, lactation, and ejaculation, while water balance and blood pressure are controlled primarily by AVP, with OXT complementing its role (Horn and Swanson 2013; Armstrong 2015; Veening et al. 2015). These functional specializations of OXT and AVP MNCs are accompanied by their unique electrophysiological behaviour and responsiveness to specific physiological stimuli in vivo: OXT MNCs produce synchronized burst activity in response to suckling, whereas AVP MNCs react to changes in blood pressure by adapting phasic activity patterns (Poulain et al. 1977; Brown et al. 2013).

Apart from neurohypophysis, OXT and AVP MNCs in the PVN project centrally to various brain regions (e.g., hippocampus, striatum, amygdala, and prefrontal cortex), wherein OXT and AVP act as neuromodulators and neurotransmitters (Silverman and Zimmerman 1983; Raggenbass 2001; Knobloch et al. 2012; Stoop 2012; Hernández et al. 2015). Additionally, independent of axonal release, OXT and AVP can be released from dendrites and somata of MNCs to exert autoregulatory roles and act locally within the hypothalamus (Ludwig et al. 2002; Ludwig and Leng 2006). Central release of OXT and AVP is involved in the regulation of social and parenting behaviours as well as learning and emotional processing (Meyer-Lindenberg et al. 2011; Bosch and Neumann 2012; Baribeau and Anagnostou 2015; Caldwell 2017). OXT and AVP are also produced by parvocellular PVN neurons; however, these subpopulations have different projection patterns and are involved in different functions (e.g., stress reaction, autonomic response, and pain regulation) (Koshimizu et al. 2012; Eliava et al. 2016; Jurek and Neumann 2018).

MNCs are among the most extensively studied hypothalamic neurons, with a plethora of data describing their physiology and function both in vivo and ex vivo. As an excellent experimental model for studying neuronal activity, MNCs have contributed to our understanding of fundamental phenomena in neuroendocrinology and neuroscience, such as axonal/somatodendritic peptide release or generation and regulation of different firing patterns (Poulain and Wakerley 1982; Renaud and Bourque 1991; Brown et al. 2013; Armstrong and Tasker 2014; Leng et al. 2015; Jurek and Neumann 2018).

Although several attempts to describe electrophysiological differences between OXT and AVP MNCs ex vivo have been made, only a few individual characteristics have been reported. The first difference observed was that depolarizing after-potentials following a train of spikes are displayed by a greater percentage of AVP rather than OXT MNCs in the SON (Armstrong et al. 1994). Additionally, the following features were claimed to be characteristic of only OXT MNCs in the SON: sustained outwardly rectifying potassium current (SOR, Stern and Armstrong 1995, 1997), rebound depolarization at the offset of the hyperpolarizing current injection (Stern and Armstrong 1995), and an inwardly rectifying hyperpolarization-activated current (Hirasawa et al. 2003; Zampronio et al. 2010). Importantly, none of these features allows for reliable discrimination between the two MNC types (Li et al. 2007; da Silva et al. 2015).

Notably, the physiological roles of OXT and AVP are sex-specific, with OXT action during labour and lactation being the most striking example (Wakerley and Lincoln 1973; Hatton and Wang 2008). It is now clear that both peptides differentially modulate a wide range of sex-specific social behaviours (e.g., pair bonding, parenting, aggression, and social recognition), where OXT and AVP can exert opposing effects between sexes or have a stronger or no effect in one sex or the other. These functional differences are accompanied by the sex-specific anatomy of the OXT and AVP brain systems. The high species specificity of these sex differences implies their roles in varying social structures among species (de Vries 2008; Nephew 2012; Knobloch and Grinevich 2014; Dumais and Veenema 2016; Bangasser and Wicks 2017; Bendesky et al. 2017; Bredewold and Veenema 2018).

Despite the sex differences identified and the many pioneering behavioural studies published, no comprehensive analysis of male and female MNC electrophysiology has been reported. Considering species-specific sex differences in the anatomy of the OXT and AVP systems, the present study aimed to thoroughly characterize (1) the number and anatomical distribution of OXT- and AVP-immunoreactive (ir) neurons within the identified PVN subnuclei and (2) the electrophysiology of OXT and AVP MNCs in male and female Sprague-Dawley rats. These experiments were performed utilizing immunostaining techniques and ex vivo whole-cell recordings combined with subsequent examination of the neurochemical nature of recorded neurons.

The obtained results indicate differences in the number of OXT- and AVP-ir neurons within the PVN area as well as sex differences in the number of PVN MNCs. Moreover,

we identified several novel differences in electrophysiological properties between putative OXT and AVP MNCs that, for the first time, allow for unambiguous discrimination in ex vivo recordings and indicate their distinct nature despite their common developmental origin (Karim and Sloper 1980). Importantly, with no striking sex differences observed, our results rule out the endogenous electrophysiological features of OXT and AVP MNCs as a prevailing source of the distinct actions of these neuropeptides in females and males, further strengthening the roles of OXT and AVP systems anatomy and their receptor expression patterns in related sex-specific behaviours.

Methods

Ethical approval

All procedures performed in studies involving animals were approved by the 1st Local Ethical Commission on Animal Research (Krakow, Poland) and conducted in accordance with the directive 2010/63/EU of the European Parliament and of the Council of 22 September 2010 on the protection of animals used for scientific purposes and the Act on the Protection of Animals Used for Scientific or Educational Purposes of 15 January 2015. All efforts were made to minimize suffering and to reduce the number of animals used.

Animals

Male and female Sprague-Dawley rats were bred and housed in a conventional animal facility at the Institute of Zoology and Biomedical Research at the Jagiellonian University in Krakow. Rats were kept in plastic cages lined with wooden bedding under constant environmental conditions (21 ± 2 °C) and maintained on a 12–12 light–dark cycle (light on at 08:00 h) with ad libitum access to fresh water and standard laboratory rodent chow. From the age of 4 weeks, rats were separated from dams and kept in the same-sex cages (3–8 per cage) until the experiment. Four-month-old adult (McCutcheon and Marinelli 2009) rats were used for immunostaining experiments; 6– 8-week-old young adult (McCutcheon and Marinelli 2009) rats were used for patch-clamp experiments.

Reagents

All reagents for the phosphate-buffered saline (PBS) solution, artificial cerebrospinal fluid, and intrapipette solution (apart from biocytin, purchased from Tocris Bioscience, Bristol, UK, 3349 or Sigma-Aldrich, B4261) were purchased from Sigma-Aldrich (Darmstadt, Germany).

The suppliers of the immunostaining reagents were as follows: 36–38% formaldehyde solution, POCH, Gliwice, Poland, 432173111; Triton X-100, Sigma-Aldrich; normal donkey serum (NDS), Abcam, Cambridge, UK, ab7475; avidin–fluorescein conjugate, Sigma-Aldrich, 94091; mouse anti-OXT antibody, Abcam, ab78364, RRID:AB_1603099 or Merck Millipore, Darmstadt, Germany, MAB5296, RRID:AB_2157626; rabbit anti-AVP antibody, Abcam, ab39363, RRID:AB_778778; anti-mouse Alexa Fluor 647-conjugated antibody, Jackson ImmunoResearch, West Grove, PA, USA, 715-606-150, RRID:AB_2340865; anti-rabbit Cy3-conjugated antibody, Jackson ImmunoResearch, 711-165-152, RRID:AB_2307443; and Fluoroshield with DAPI, Sigma-Aldrich, F6057. Primary antibodies and NDS were aliquoted and stored at − 20 °C; secondary antibodies were aliquoted and stored at − 80 °C.

The suppliers of the electrophysiology reagents were as follows: tetrodotoxin citrate (TTX), Abcam, ab 120055 and Tocris Bioscience, 1069; 2-amino-5-phosphopentanoic acid (DL-AP5) Tocris Bioscience, 0105; 6-cyano-7-nitroquinoxaline-2,3-dione disodium salt (CNQX) Tocris Bioscience, 1045; and bicuculline methiodide, Sigma-Aldrich, 14343. All drugs were dissolved in deionized water, aliquoted and stored at − 20 °C.

Tissue preparation, immunostaining, and reconstruction of PVN neuron distribution

Male ($n = 4$) and female ($n = 6$) Sprague-Dawley rats (adult 4 months old) were sedated with isoflurane (AErrane, Baxter, Warsaw, Poland), anaesthetized with pentobarbital (IP, 1.5 ml/kg, Morbital, Biowet, Pulawy, Poland), and sacrificed by transcardial perfusion with 200 ml of PBS followed by 200 ml of a 4% formaldehyde solution in PBS (made fresh from a 38% solution). After overnight post-fixation in a 4% formaldehyde solution (at 4 °C), the brains were cut into coronal sections (50 µm thick) on a vibrating microtome (Leica VT1000 S, Leica Instruments, Heidelberg, Germany).

Ten consecutive sections containing magnocellular PVN divisions [corresponding to stereotactic atlas plates from − 1.44 to − 1.92 mm caudal to bregma (Paxinos and Watson 2007)] were selected from each brain and stained for either OXT or AVP (every second section, five sections for each staining) as previously described (Kania et al. 2017). Briefly, after blocking and permeabilization for 1 h at room temperature (10% NDS, 0.3% Triton X-100 in PBS solution), the sections were incubated with primary antibodies for 72 h at 4 °C [2% NDS, 0.3% Triton X-100 in PBS solution containing a mouse anti-OXT antibody (1:10 000) or a rat anti-AVP antibody (1:500)]. The specificities of the widely validated primary antibodies used (Zhao et al. 2017; Roy et al. 2018; Barna et al. 2019) were verified by competitive ELISA according to the manufacturer's instructions. Moreover, double immunostaining of the PVN slices against OXT and AVP after patch-clamp recordings (described below)

revealed negligible number of double-labelled neurons, further confirming good specificity of antibodies. Finally, the sections were incubated with secondary antibodies for 24 h at 4 °C [2% NDS in PBS solution containing a donkey anti-mouse Alexa Fluor 647-conjugated antibody (1:400) or a donkey anti-rabbit Cy3-conjugated antibody (1:400)]. Each step was followed by washing with PBS. Stained sections were mounted and coverslipped with Fluoroshield™ containing DAPI. Images were collected using a confocal laser microscope (LSM710 on Axio Observer.Z1, Zeiss, Gottingen, Germany) with the EC Plan-Neofluar 20×/0.50 M27 objective with 0.6× digital zoom. AVP- and OXT-ir neuron distributions within the PVN area were assessed based on z-stack images (2048 × 2048). OXT- and AVP-ir neurons were counted unilaterally and assigned to an anatomical subdivision according to the rat brain atlas (Paxinos and Watson 2007) using ZEN 2.1 (Zeiss, Gottingen, Germany; RRID:SCR_013672) and CorelDraw X8 (Corel Corporation, Ottawa, Canada; RRID:SCR_014235) software. All cell counts were done manually by examining one optical plane after another. Cells were included in the count if they: (1) were located in the PVN, (2) exhibited a reliable OT or AVP staining pattern (faintly stained, questionable cells were excluded), and (3) contained a nucleus (DAPI-positive signal). Depending on its location, each cell was assigned to a defined subdivision of the PVN. Care was taken not to allocate given cell in more than one subdivision. If a cell happened to be located on the boundary of two sub-regions, it was assessed and included in the sub-region containing the major part of this cell. Each z-stack image used for the counting contained the whole area of interest (unilateral coronal image of PVN); therefore, there was no need for edge effect correction. Furthermore, collecting every second 50 µm-thick section for given immunostaining (even sections for OXT staining, odd for AVP staining, respectively), eliminated the probability of presence of the same stained cell body on more than one brain section.

Patch-clamp experiments and post-recording immunostaining

Patch-clamp recordings were performed according to previously described methods (Kastman et al. 2016; Kania et al. 2017). Briefly, male and female Sprague-Dawley rats (young adult, 6–8 weeks old) were anaesthetized with isoflurane and decapitated between zeitgeber times (ZT) 2 and 3. Brains were collected and cut into 250-µm-thick coronal slices on a vibrating microtome (Leica VT1000 S) in carbogenated ice-cold, sucrose-rich, low-sodium, high-magnesium artificial cerebrospinal fluid (ACSF), comprising the following (in mM): 185 sucrose, 25 $NaHCO_3$, 3 KCl, 1.2 NaH_2PO_4, 2 $CaCl_2$, 10 $MgSO_4$, and 10 glucose (pH 7.4; osmolality 290–300 mOsmol kg^{-1}). PVN-containing sections were bisected along the third ventricle and transferred to an incubation chamber containing carbogenated, warm (32 °C) ACSF comprising the following (in mM): 118 NaCl, 25 $NaHCO_3$, 3 KCl, 1.2 NaH_2PO_4, 2 $CaCl_2$, 2 $MgSO_4$, and 10 glucose (pH 7.4; osmolality 290–300 mOsmol kg^{-1}). After at least 90 min of recovery, slices were transferred to the submerged recording chamber, wherein the tissue was continuously perfused (2 ml min^{-1}) with carbogenated, warm (32 °C) ACSF of the same composition.

Recording micropipettes (5–7 MΩ resistance), pulled on a horizontal puller (P-1000, Sutter Instruments, Novato, CA, USA) from borosilicate glass capillaries (Sutter Instruments), were filled with a solution containing (in mM) 145 potassium gluconate, 1.3 $MgCl_2$, 4 Na_2ATP, 0.4 Na_3GTP, 5 EGTA, 10 HEPES (pH 7.3; osmolality 290–300 mOsmol kg^{-1}), and biocytin (0.05%), allowing for subsequent immunofluorescent identification of recorded neurons. The calculated liquid junction potential for ACSF and the intrapipette solution was + 15 mV, and this value was subtracted from the data.

PVN neurons were localized and approached using a light microscope equipped with video-enhanced infrared differential interference contrast (Axio Examiner.D1, Zeiss, Gottingen, Germany). Cell-attached and whole-cell configurations were obtained under visual control with mouth suction. The SEC 05 LX amplifier (NPI, Tamm, Germany), Micro 1401 mk II [Cambridge Electronic Design (CED), Cambridge, UK] converter, and Signal and Spike2 software (CED, RRID:SCR_017081, RRID:SCR_000903) were used for signal recording (low-pass filtered at 3 kHz and digitized at 20 kHz) and data acquisition. All drugs were delivered via a bath perfusion system.

After recording, slices were fixed with 4% formaldehyde (overnight at 4 °C) and immunostained according to a previously described protocol (Kania et al. 2017) to examine the neurochemical contents (OXT/AVP) of recoded neurons. Briefly, after blocking and permeabilization for 3 h at room temperature or 24 h at 4 °C (10% NDS, 0.3% Triton X-100 in PBS solution), sections were incubated with primary antibody mixtures supplemented with an avidin–fluorescein conjugate for 48–72 h at 4 °C [2% NDS, 0.3% Triton X-100 in PBS solution containing a mouse anti-OXT antibody (1:5000/1:10 000 depending on the antibody used), rat anti-AVP antibody (1:500/1:5000 depending on the antibody used), and avidin–fluorescein conjugate (1:200)]. Finally, sections were incubated with secondary antibody mixtures for 24 h at 4 °C (2% NDS in PBS solution containing a donkey anti-mouse Alexa Fluor 647-conjugated antibody (1:400) and a donkey anti-rabbit Cy3-conjugated antibody (1:400). Each step was followed by washing with PBS. Stained sections were mounted, coverslipped with Fluoroshield™ containing DAPI, and imaged and analysed with a fluorescence microscope (Axio Imager.M2,

Zeiss, Gottingen, Germany). Even after successful immunostaining, the antigen of interest can be undetectable in patch-recorded neurons (due to, for e.g., the physiological state, low expression, dilution of antigen by the intrapipette solution, or disruption of the cell membrane by prolonged recording), and the lack of OXT or AVP immunoreactivity was never a prerequisite for labelling an MNC as non-OXT or non-AVP.

Electrophysiological data acquisition and analysis

All current clamp recordings were performed in normal ACSF. Stimulations were delivered from a membrane potential of − 75 mV sustained with continuous current injections.

Single action potentials (APs) evoked by a 2-ms-long depolarizing current pulse were analysed using the Signal script provided on the CED website to calculate several AP features: (1) threshold, (2) amplitude (from threshold to AP peak), (3) 10–90 rise time, (4) half width, (5) hyperpolarizing after-potential (HAP) trough (minimum membrane potential value after AP peak), and (6) time between AP peak and HAP trough.

Several membrane parameters were assessed based on voltage response to current steps or ramp and analysed using custom Signal scripts. The voltage response to a 50 pA current pulse (500 ms) was utilized to calculate the following: (1) the membrane time constant, which was determined by fitting a single exponential to the charging phase of the voltage response; (2) the membrane resistance, which was calculated based on the maximum amplitude of the voltage response, assuming an ohmic current–voltage (I–V) relationship; and (3) the membrane capacitance, which was calculated as the quotient of the time constant and resistance. (4) The voltage sag was measured from the voltage response to a − 140 pA hyperpolarizing current step (500 ms). The voltage response to current ramp stimulation (0–1 nA in 1 s) was used to determine (5) the rheobase, which was measured as the ramp current value at the moment of reaching the AP threshold (6), which was determined as the point corresponding to the steepest slope of the third derivative of the AP waveform. (7) Maximal spiking frequency was calculated using the minimal interspike interval measured during ramp current stimulation. (8) The voltage–current relationship was traced based on steady-state voltage responses to decremental hyperpolarizing current pulses from − 140 to − 10 pA (10 pA decrement, pulse duration 500 ms, and 5 s between steps). (9) Neuronal excitability (input–output relationship) was measured as the number of spikes elicited by incremental depolarizing current pulses from + 10 to + 140 pA (10 pA increment, pulse duration 500 ms, and 5 s between steps). Only current steps triggering APs were used to characterize the input–output relationship.

Voltage clamp stimulations were delivered from a holding potential of − 75 mV in the presence of TTX (0.5 µM, to block AP generation) and antagonists of ionotropic glutamate and GABA receptors (10 µM CNQX, 50 µM DL-AP5, and 20 µM bicuculline, respectively, to block postsynaptic currents). Voltage steps from − 120 to + 10 mV (10 mV change, pulse duration 500 ms, and 3 s between steps) were used to measure the I–V relationships of the steady-state current. Linear or nonlinear regression for parameters acquired in the current (excitability and steady-state voltage I–V relationship) and voltage clamp mode (steady-state current I–V relationship) was calculated in R (R Core Team 2018, RRID:SCR_001905).

Spontaneous synaptic activity was measured at a holding potential of − 50 mV. Since the calculated reversal potential for Cl^- currents equalled − 90.51 mV, at a set holding potential, outward events represented inhibitory postsynaptic currents, whereas inward events represented excitatory postsynaptic currents (sIPSCs and sEPSCs, respectively). The nature of postsynaptic currents was verified using glutamate [CNQX (10 µM), DL-AP5 (50 µM), and GABA (bicuculline, 20 µM) receptor antagonists (data not shown)]. Two hundred second-long recordings of spontaneous inhibitory and excitatory postsynaptic currents from each MNC were analysed using Mini Analysis software (Synaptosoft Inc., Fort Lee, NJ, USA). Events were manually detected to measure the following parameters: (1) frequency and interevent interval, (2) mean rise time, (3) mean amplitude, and (4) decay time constant of the averaged current trace.

Statistics

Statistical analyses of anatomical data were performed among four groups of neurons [male oxytocin-ir (OXT-IR♂), male arginine vasopressin-ir (AVP-IR♂), female oxytocin-ir (OXT-IR♀), and female arginine vasopressin-ir (AVP-IR♀)], whereas electrophysiological parameters of MNCs were compared among male putative oxytocin (OXT♂), male putative arginine vasopressin (AVP♂), female putative oxytocin (OXT♀), and female putative arginine vasopressin (AVP♀) neurons. In a subset of electrophysiological parameters (AP features and membrane properties: resistance, time constant, capacitance, rheobase, AP threshold, maximal spiking frequency, and voltage sag in response to hyperpolarizing current pulse), outliers were detected using the ROUT method ($Q = 5\%$) and excluded from the analysis. Data were assessed as normally distributed and analysed by two-way ANOVA. Robust differences in variations between putative OXT and AVP MNCs in time from the AP peak to the HAP trough prevented reliable two-way ANOVA comparisons. The time from the AP peak to the HAP trough parameters was compared between male and female putative OXT MNCs as well as between male and female

putative AVP MNCs using Student's *t* test. Data sets for (1) AP parameters and (2) selected membrane properties were processed using principal component analysis (PCA). The obtained principal components were analysed analogically to the rest of the electrophysiological data and additionally tested using nested two-way ANOVA to reveal potential random effects of the animals from which the MNC parameters were obtained. All differences were considered statistically significant at $p < 0.05$. Data analysis was performed using GraphPad Prism for Windows (RRID:SCR_002798) and R (R Core Team 2018). Graphics were made using GraphPad Prism, R, and CorelDraw software.

Results

Paraventricular nucleus AVP-ir neurons are more numerous than OXT-ir neurons

Coronal sections through the PVN obtained from male and female rats were immunostained for either OXT or AVP. OXT- and AVP-ir neurons were counted, and numbers were compared among whole PVNs as well as among the following anatomically distinct PVN subdivisions: the dorsal cap (PaDC), the ventral part (PaV), the medial parvocellular part (PaMP), the lateral magnocellular part (PaLM), and the medial magnocellular part (PaMM) (Fig. 1a). ANOVA showed that the total number of PVN AVP-ir neurons was significantly higher than the total number of PVN OXT-ir cells in both sexes. Moreover, males had significantly more OXT-ir and AVP-ir neurons than females, as shown by significant sex differences and lack of interaction between sex and peptide content. Regarding the PVN subdivisions, more AVP- than OXT-ir neurons were present in PaDC, PaV, and PaLM than in the other regions in both sexes. Significant sex differences in immunoreactive cell numbers were observed only in PaMM, with more neurons (OXT and AVP) being observed in males. No significant interactions between the PVN cell peptide content and sex were observed among the PVN subdivisions (Fig. 1d). Detailed data regarding the number of AVP- and OXT-ir cells as well as statistical test results are shown in Online resource Table 1.

Identification of PVN magnocellular neurosecretory cells

Electrophysiological differences between PVN neuronal populations allow for the identification of MNCs based on (1) the presence of transient outward rectification mediated by a robust A-type potassium current (Fig. 2a) and (2) the lack of low-threshold spikes generated by T-type calcium currents (characteristic feature of parvocellular neurons) (Luther and Tasker 2000). According to these criteria, data from 261 putative MNCs recorded in the brain slices obtained from 90 young adult Sprague-Dawley rats (35 males and 55 females) were included in the present study. The vast majority of recorded MNCs were localized in the PaMM and PaLM regions of the PVN.

MNCs were further identified as putative OXT or AVP based on the post-recording immunostaining (122 and 82 MNCs, respectively) and/or on striking differences in the time course and shape of the HAP following a single AP (see below, Fig. 2b, c). Altogether, 261 MNCs included in this study were assigned to one of four groups: male putative oxytocin (OXT♂, $n = 50$), male putative vasopressin (AVP♂, $n = 47$), female putative oxytocin (OXT♀, $n = 97$), and female putative vasopressin (AVP♀, $n = 67$).

The first set of experiments was aimed at characterizing the APs and passive and active membrane properties of PVN MNCs. Overall, 107 putative OXT neurons (36 male and 71 female) and 76 putative AVP (27 male and 49 female) neurons were recorded in normal ACSF in the current clamp mode.

OXT and AVP MNC action potentials are highly distinctive

Two strikingly distinct shapes of HAPs following induced single APs were observed among the recorded MNCs. Based on post-recording immunofluorescence staining, these distinct waveforms could be assigned to either OXT-ir (51 out of 62 successfully stained MNCs displaying HAPs with slow kinetics were OXT-ir and none were AVP-ir) or AVP-ir MNCs (28 out of 32 successfully stained MNCs HAPs with fast kinetics were AVP-ir and none were OXT-ir, Fig. 2b). These differences in the AP waveform between OXT-ir and AVP-ir MNCs allowed for further unequivocal differentiation between MNCs lacking immunofluorescent identification.

ANOVA revealed additional significant differences between putative OXT and AVP MNC APs with OXT MNCs having longer 10–90 rise times and half widths as well as more depolarized HAP troughs than AVP MNCs. No differences in the AP threshold or amplitude values were observed. No significant sex differences or interactions between sex and peptide content were observed among all the ANOVA comparisons. Sex differences in the times from the AP peaks to the HAP troughs of putative OXT MNCs were revealed by Student's *t* test, with males having significantly slower kinetics than females. No such sex differences were observed in putative AVP MNCs (Fig. 3). The mean values of the analysed AP features as well as the statistical tests used and their results are shown in Online resource Table 2.

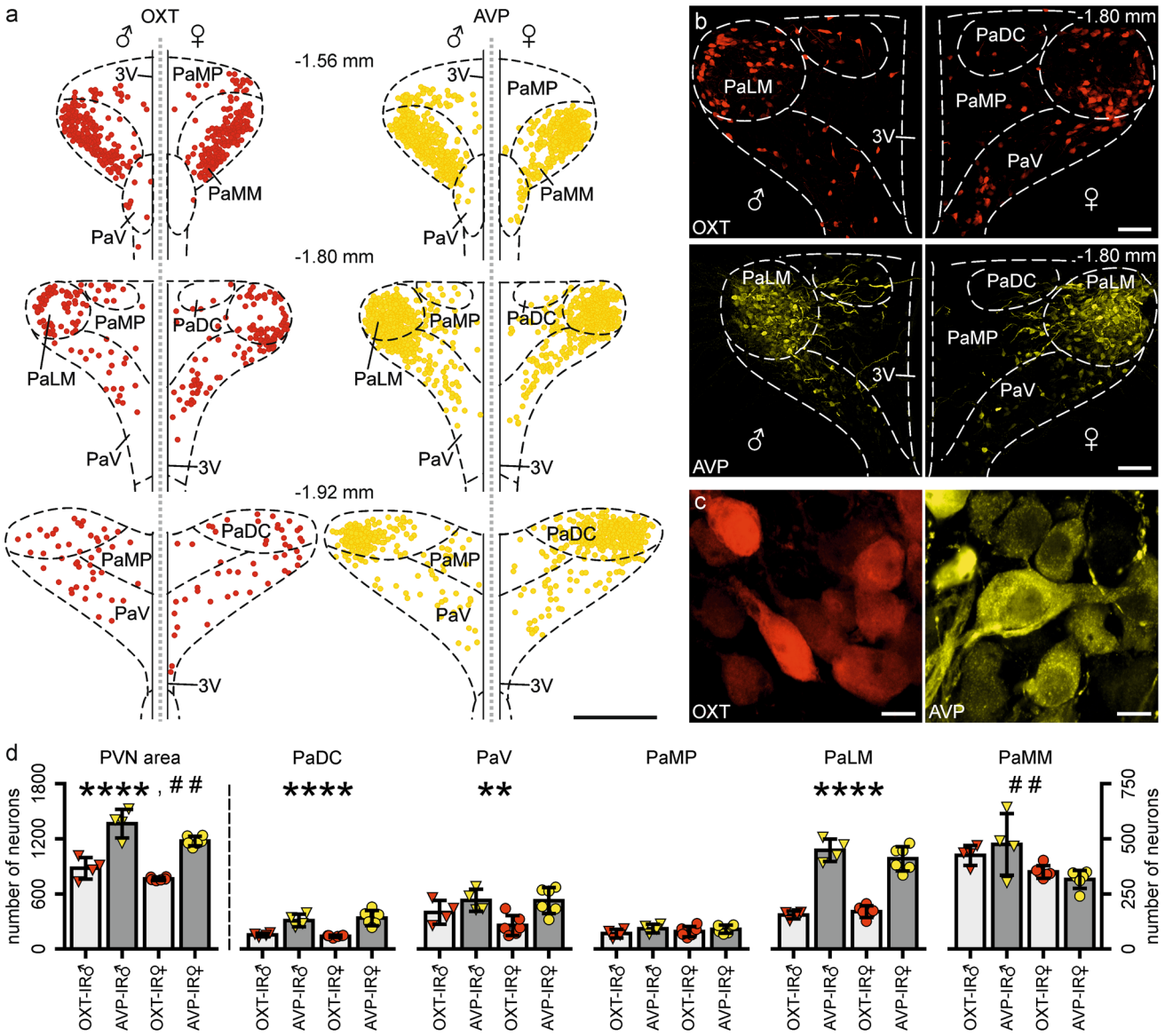

Fig. 1 Distributions and numbers of OXT- and AVP-ir neurons in the PVN area. **a** Schematic reconstruction of the distributions of OXT- (red circles) and AVP-ir (yellow circles) neurons on selected coronal sections of the rat PVN area. The left and right plates represent male and female PVNs, respectively. The distance from bregma is indicated for each section. Scale bar: 400 µm. **b** Confocal microscope projection images of coronal hypothalamic sections at the level of PVN illustrating OXT- (top, red) and AVP-ir (bottom, yellow) neuron distribution. The left and right images represent male and female PVNs, respectively. The distance from bregma is indicated. Scale bar: 100 µm. **c** High magnification confocal projection images illustrating OXT- (left, red) and AVP-ir (right, yellow) PVN neurons. Scale bar: 10 µm. **d** Strip charts with bars showing the numbers of neurons in the whole PVN area (left) and its anatomical subdivisions (right): male OXT-ir (OXT-IR♂), male AVP-ir (AVP-IR♂), female OXT-ir (OXT-IR♀), and female AVP-ir (AVP-IR♀). Bars and whiskers represent means and SDs. Symbols indicate statistical significance in two-way ANOVA: differences between the numbers of OXT-ir and AVP-ir neurons are marked as ** ($p < 0.01$) and **** ($p < 0.0001$); differences between the numbers of male and female-ir neurons are marked as $^{\#\#}$ ($p < 0.01$). *3V* third ventricle; paraventricular nucleus subdivisions: *PaDC* dorsal cap, *PaLM* lateral magnocellular part, *PaMM* medial magnocellular part, *PaMP* medial parvicellular part, *PaV* ventral part

Putative OXT and AVP MNCs display different passive and active membrane properties

Several parameters characterizing the membrane electrophysiology of PVN MNCs were obtained using incremental current steps and/or fast current ramp stimulations (Fig. 4a, b). ANOVA revealed significant differences between putative OXT and AVP MNCs, with OXT MNCs being characterized by a higher membrane resistance and maximal spiking frequency as well as a lower membrane capacitance,

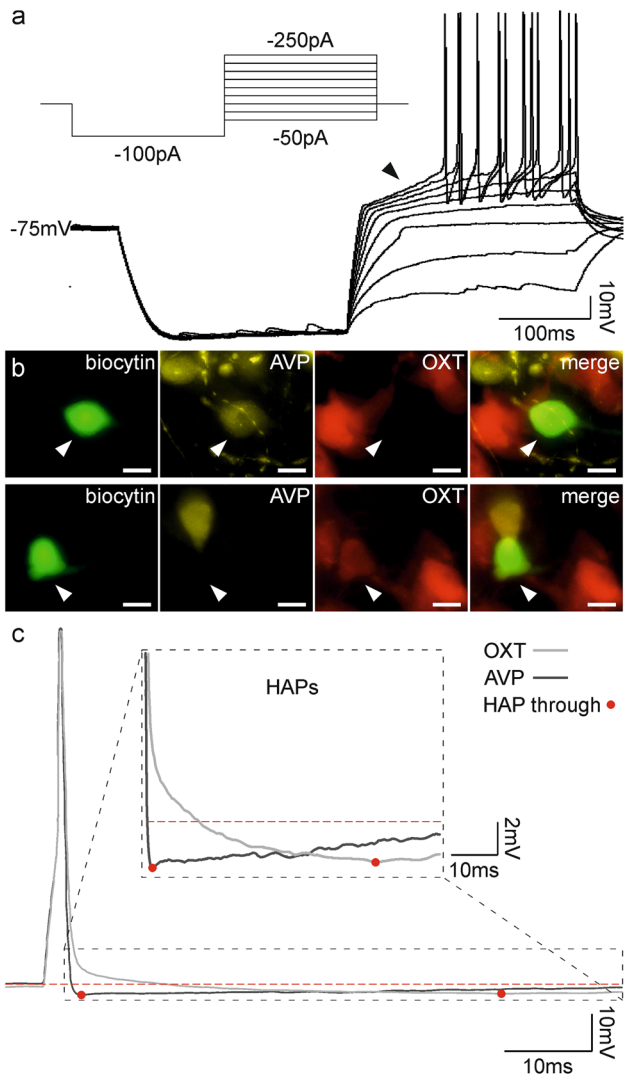

Fig. 2 Identification of OXT and AVP PVN magnocellular neurosecretory cells. **a** Exemplary current clamp protocol (upper trace) used for the electrophysiological identification of PVN neurons. MNCs were identified by the presence of a transient outward rectification causing a delay to the first action potential (lower trace, black arrowhead) after being depolarized from the hyperpolarized state of the membrane. **b** Post-recording immunofluorescent identification of MNCs: (top) series of fluorescence projection images illustrating biocytin-filled AVP-ir MNCs (white arrowhead); (bottom) series of fluorescence projection images illustrating biocytin-filled OXT-ir MNCs (white arrowhead). Scale bar: 10 µm. **c** Exemplary APs of OXT (light grey) and AVP (dark grey) MNCs showing differences in HAP kinetics. Zoom in on HAPs: OXT MNCs have slower HAP kinetics, whereas AVP MNC HAPs are characterized by fast overshoots. Spikes were elicited with a brief (2 ms) current injection from a membrane potential of − 75 mV

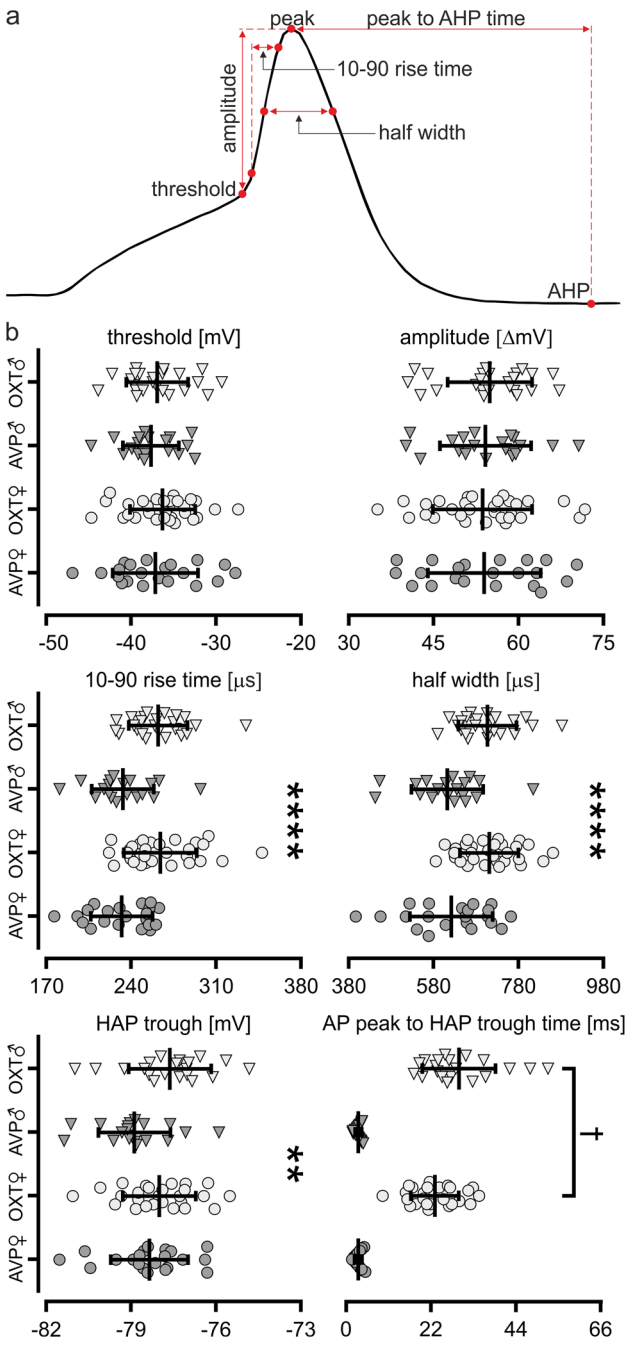

Fig. 3 Action potential parameters of PVN magnocellular neurosecretory cells. **a** Exemplary waveform of a single, evoked action potential illustrating measured properties. Spikes were elicited from a membrane potential of − 75 mV with a brief (2 ms) current injection. **b** Strip charts showing the action potential parameters of four MNC groups: male putative oxytocin (OXT♂), male putative vasopressin (AVP♂), female putative oxytocin (OXT♀), and female putative vasopressin (AVP♀) neurons. Lines and whiskers represent means and SDs. Symbols indicate statistical significance in two-way ANOVA: differences between putative OXT and AVP MNCs are marked as ** ($p < 0.01$) and **** ($p < 0.0001$). Unpaired Student's t test (marked as †, $p < 0.05$) revealed that male putative OXT MNCs display a significantly longer AP peak to HAP over time than female putative OXT MNCs

rheobase, AP threshold, and voltage sag amplitude. No differences in time constants were observed. Significant sex differences were found in only one parameter, with male MNCs being characterized by a higher membrane resistance than female MNCs. No significant interactions of sex

and peptide content were observed. The mean values of the analysed membrane parameters as well as the statistical tests used and their results are shown in Online resource Table 3.

Both the steady-state voltage in response to decremental hyperpolarizing current steps and the number of spikes in response to incremental depolarizing current steps were characterized by a strong linear relationship (mean R^2 equalled 0.98 and 0.97, respectively, Fig. 4d). Therefore, the steady-state voltage I–V relationships and excitability curves were characterized and compared using the linear regression curve slope and *y* intercept. Again, ANOVA revealed differences between putative OXT and AVP MNCs. Steady-state voltage I–V curve *y* intercepts were significantly lower in putative OXT than in AVP MNCs. No differences in curve slopes were reported. OXT MNCs were also characterized by higher excitability curve slopes (stronger gain) and *y* intercepts than AVP MNCs. No significant sex differences between MNCs and no interactions between sex and peptide content were observed. The mean values of the analysed linear regression coefficients as well as the statistical tests used and their results are shown in Online resource Table 4.

The steady-state current–voltage relationship does not differ among PVN MNCs

A second set of experiments aimed at investigating PVN MNC membrane properties was carried out in ACSF containing TTX as well as CNQX, DL-AP5, and bicuculline to block sodium AP generation and synaptic activity, respectively. The I–V relationships of the steady-state current were measured using a series of incremental voltage steps (Fig. 4c) in 35 putative OXT (13 male and 22 female) and 29 putative AVP (16 male and 13 female) MNCs. The steady-state current I–V relationship was highly nonlinear and strongly outwardly rectifying in all MNCs. Therefore, polynomial curves were fitted to the data using nonlinear regression models (mean $R^2 = 0.998$, Fig. 4d). ANOVA showed no significant differences between intercepts and equation coefficients among MNCs. Data regarding polynomial regression curve coefficients and the statistical tests used to compare them are presented in Online resource Table 4.

Principal component analysis shows differences in OXT and AVP MNC electrophysiology

Complete data sets regarding either the AP characteristics of MNCs or their active and passive membrane properties were further transformed and analysed using PCA (Fig. 5). PCA was performed on the properties of the APs, including all of the following aforementioned parameters: (1) threshold, (2) amplitude, (3) 10–90 rise time, (4) half width, (5) HAP value at the trough, and (6) time from the AP peak to the HAP trough. The first three principal components (PCs), explaining 85% of the observed variance, were considered. Significant differences between putative OXT and AVP MNCs were observed in all three PCs, with no sex differences or interaction between sex and peptide content being reported (Fig. 5b). PCA of membrane property parameters considered only those characterized by at least a 'medium' effect size (Cohen's *d*: defined as the difference between two means: OXT vs. AVP MNCs, divided by a standard deviation). These parameters included (1) membrane resistance, (2) membrane capacitance, (3) steady-state voltage I–V curve intercept, (4) excitability curve slope, (5) AP threshold, and (6) rheobase. Again, the first three PCs, explaining 76.5% of the observed variance, were considered. Significant differences between putative OXT and AVP MNCs were observed in first PC, with no sex differences or interaction between sex and peptide content being reported (Fig. 5d). To address the potential random effects of variability between animals, the PCs were additionally analysed using nested two-way ANOVA. No significant random effects were observed, and the reported variances between animals were always lower than the residual variances, indicating little influence of variability between animals on the reported results. Moreover, no statistically significant differences between these two models (two-way ANOVA vs. nested two-way ANOVA) were reported.

The synaptic input properties of putative OXT and AVP MNCs differ

The third and final set of recordings was aimed at characterizing the spontaneous synaptic input to the PVN MNCs. A subset of MNCs [24 putative OXT (12 male and 12 female) and 23 putative AVP (12 male and 11 female)] was voltage-clamped at − 50 mV to measure spontaneous excitatory and inhibitory synaptic events (Fig. 6a) in normal ACSF. Overall, the inhibitory synaptic activity recorded from PVN MNCs was significantly more robust than the excitatory activity (sIPSC vs sEPSC frequency: 9.19 ± 6.86 vs. 1.11 ± 0.51 Hz in males and 7.58 ± 5.67 vs. 1.06 ± 0.83 Hz in females, two-way ANOVA, synaptic activity type (sIPSCs vs. sEPSCs): $p < 0.0001$, sex: $p > 0.05$, interaction: $p > 0.05$). Moreover, ANOVA revealed differences between putative OXT and AVP MNCs for almost all the measured parameters. The sIPSCs of OXT MNCs were characterized by a higher frequency, lower amplitude and slower rise time, and decay time constant than AVP MNCs, whereas the sEPSCs of OXT MNCs had a higher frequency and amplitude but a slower rise time than AVP MNCs. No significant differences were observed in the sEPSC decay time constant. ANOVA showed no significant sex differences or interaction between sex and peptide content in any of the analysed parameters (Fig. 6b). The mean values of the synaptic

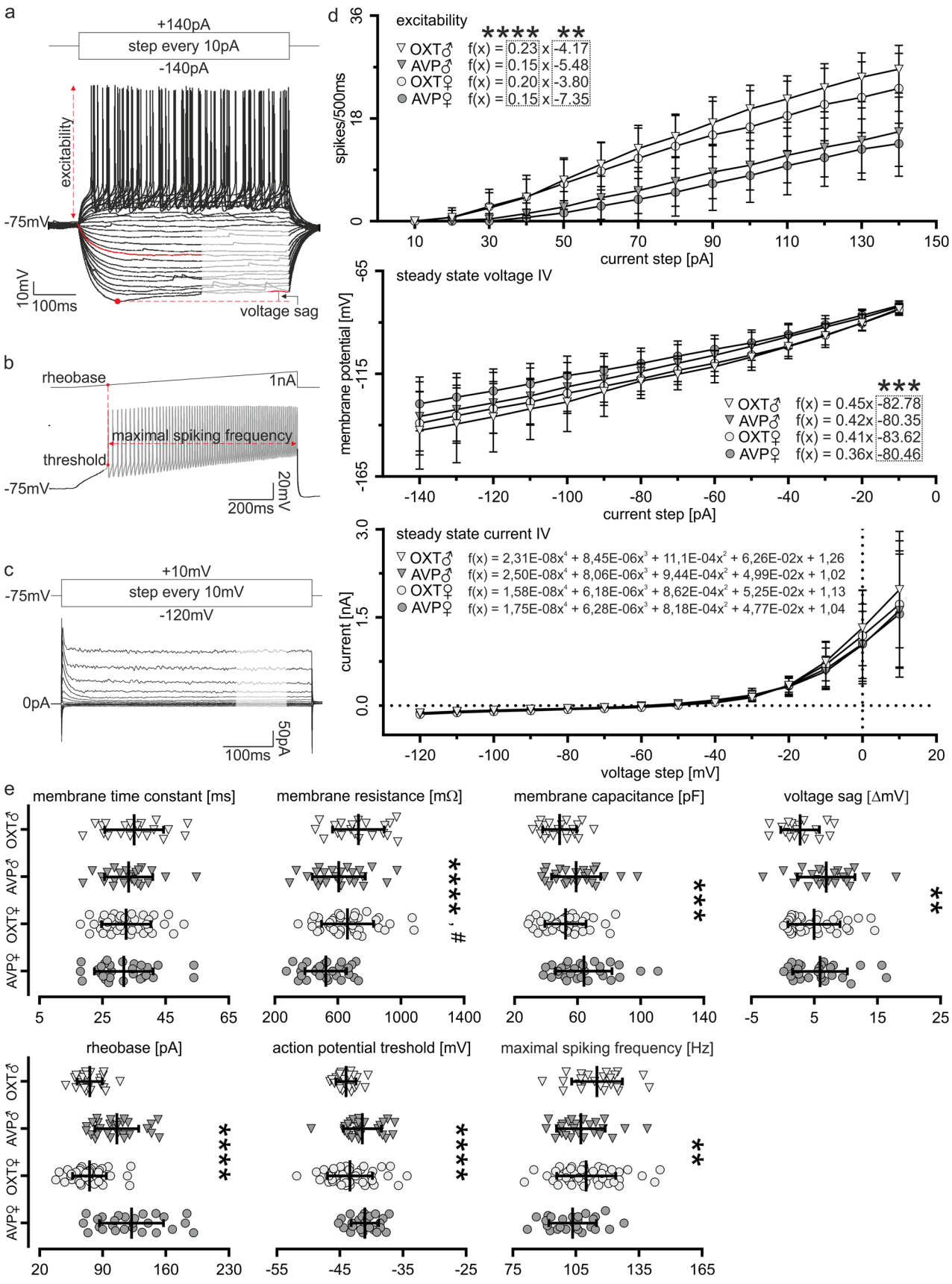
a
+140pA
step every 10pA
-140pA
excitability
-75mV
10mV
100ms
voltage sag
b
rheobase
1nA
maximal spiking frequency
threshold
-75mV
20mV
200ms
c
+10mV
-75mV
step every 10mV
-120mV
0pA
50pA
100ms
d
excitability
**** **
OXT♂ f(x) = 0.23 x -4.17
AVP♂ f(x) = 0.15 x -5.48
OXT♀ f(x) = 0.20 x -3.80
AVP♀ f(x) = 0.15 x -7.35
spikes/500ms
current step [pA]
steady state voltage IV
***
OXT♂ f(x) = 0.45x -82.78
AVP♂ f(x) = 0.42x -80.35
OXT♀ f(x) = 0.41x -83.62
AVP♀ f(x) = 0.36x -80.46
membrane potential [mV]
current step [pA]
steady state current IV
OXT♂ f(x) = 2,31E-08x⁴ + 8,45E-06x³ + 11,1E-04x² + 6,26E-02x + 1,26
AVP♂ f(x) = 2,50E-08x⁴ + 8,06E-06x³ + 9,44E-04x² + 4,99E-02x + 1,02
OXT♀ f(x) = 1,58E-08x⁴ + 6,18E-06x³ + 8,62E-04x² + 5,25E-02x + 1,13
AVP♀ f(x) = 1,75E-08x⁴ + 6,28E-06x³ + 8,18E-04x² + 4,77E-02x + 1,04
current [nA]
voltage step [mV]
e
membrane time constant [ms]
membrane resistance [mΩ]
membrane capacitance [pF]
voltage sag [ΔmV]
rheobase [pA]
action potential treshold [mV]
maximal spiking frequency [Hz]
OXT♂
AVP♂
OXT♀
AVP♀

◂**Fig. 4** Passive and active membrane properties of PVN magnocellular neurosecretory cells. **a** Current-step stimulation protocol (top) and voltage responses of exemplary PVN MNCs (bottom) illustrating measured properties. Voltage sag was measured from the voltage response to a − 140 pA hyperpolarizing current step. The membrane resistance, time constant, and capacitance were measured from the voltage response (red line) to a − 50 pA hyperpolarizing current step; resistance was calculated assuming an ohmic current–voltage relationship; the time constant was measured from the charging phase of the voltage response and capacitance was calculated as the resistance and time constant quotient. The voltage–current relationship was traced based on the steady-state voltage responses (marked in grey) to decremental hyperpolarizing current pulses from − 140 to − 10 pA (step every 10 pA, step duration: 500 ms, and 5 s between steps). Neuronal excitability (input–output relationship) was quantified by measuring the number of spikes elicited by depolarizing current pulses from + 10 to + 140 pA. **b** Current ramp stimulation protocol (top) and voltage response of exemplary PVN MNCs (bottom) illustrating measured properties. Rheobase was measured as the ramp current value at the moment the action potential threshold was reached. The maximal spiking frequency was calculated using the minimal interspike interval. **c** Voltage-step stimulation protocol (top) and current responses (bottom) of exemplary PVN MNCs illustrating measured steady-state membrane currents. The voltage–current relationship was traced based on the steady-state current responses (marked in grey) to voltage-step pulses from − 120 to − 10 mV (step every 10 mV, step duration: 500 ms, and 3 s between steps). **d** Line charts showing the excitability (input–output relationship, top), steady-state voltage–current relationship (middle), and steady-state current–voltage relationship of four MNC groups: male putative oxytocin (OXT♂), male putative vasopressin (AVP♂), female putative oxytocin (OXT♀), and female putative vasopressin (AVP♀) neurons. Group symbols and whiskers represent means and SDs. Lines connect consecutive means. Linear and polynomial equations describe regression curves fitted to the data in each group. Coefficients significantly different among groups are framed; symbols indicate statistical significance in two-way ANOVA: differences between putative OXT and AVP MNCs are marked as ** ($p < 0.01$), *** ($p < 0.001$), and **** ($p < 0.0001$). **e** Strip charts showing the membrane properties of four MNC groups: male putative oxytocin (OXT♂), male putative vasopressin (AVP♂), female putative oxytocin (OXT♀), and female putative vasopressin (AVP♀) neurons. Lines and whiskers represent means and SDs. Symbols indicate statistical significance in two-way ANOVA: differences between putative OXT and AVP MNCs are marked as ** ($p < 0.01$), *** ($p < 0.001$), and **** ($p < 0.0001$); differences between male and female MNCs are marked as $^{\#}$ ($p < 0.05$)

activity parameters as well as the statistical tests used and their results are shown in Online resource Table 5.

Discussion

The present study was focused on PVN OXT and AVP neuron distribution and MNC electrophysiology to search for possible features underlying functional and sex differences between OXT and AVP peptides. We described differences in the numbers of OXT- and AVP-ir PVN neurons, with the latter being more numerous in both sexes. Moreover, we revealed sex differences in the numbers of MNCs, and showed that male rats have more PVN OXT- and AVP-ir neurons than females. Importantly, we revealed several novel characteristics of putative OXT and AVP MNC electrophysiology, the most prominent being the AP shape. The novel reported differential HAP time courses, with faster kinetics in AVP rather than OXT MNCs, allowed for unequivocal identification of these cell types in ex vivo preparations. The partially distinct electrophysiological profiles of OXT and AVP MNCs (largely overlapping between males and females) described in the present study were also shown by PCA clustering. Finally, while similarities in a number of MNC electrophysiological parameters were reported, we also described sex differences in the HAP kinetics, which were slower in putative male OXT MNCs, and in membrane resistance, which was higher in male MNCs.

OXT and AVP PVN neuron numbers

In the current neuroanatomical study, we showed that, regardless of sex, there are more AVP- than OXT-ir cells in Sprague-Dawley rat PVN. Although, as the PVN is composed of MNCs as well as parvocellular neurons, both of which express OXT and AVP, our data do not ultimately depict the contributions of specific cell types in the observed difference. Earlier reports state that the numbers of PVN OXT and AVP neurons are similar in Wistar and Long Evans rat (Swaab et al. 1975; Vandesande and Dierickx 1975; Rhodes et al. 1981); reported discrepancies may, therefore, arise from strain differences. Additionally, the anterior commissural cell group, composed primarily of OXT MNCs, considered by some as part of the PVN, was not included in our analysis (Rhodes et al. 1981; Swanson and Sawchenko 1983), which may further explain the difference.

The higher number of PVN OXT-ir cells in male rather than female Sprague-Dawley rats reported in the present study does not support the majority of anatomical/expression data published to date. In the majority of species studied, a lack of sex differences in the numbers of both OXT-ir and OXT mRNA-expressing cells in the PVN or a higher number of OXT-ir PVN neurons in females is shown, as elegantly reviewed in Dumais and Veenema (2016). Reported discrepancies may arise from not only strain/species differences but also from the fact that in the present study, all PVN subnuclei were examined, as opposed to the specific, restricted regions of interest considered in many other animal and human studies. Notably, two independent studies focusing on OXT plasma levels in Sprague-Dawley rats show contradictory results: one reports higher OXT levels in males (Windle and Forsling 1993), while another reports higher levels in females (Kramer et al. 2004). Therefore, further research is needed to reach unambiguous conclusions regarding the level of this hormone in this rat strain. Importantly, a quantitative comparison of both OXT cell output and input fibre distribution between males and females is still missing.

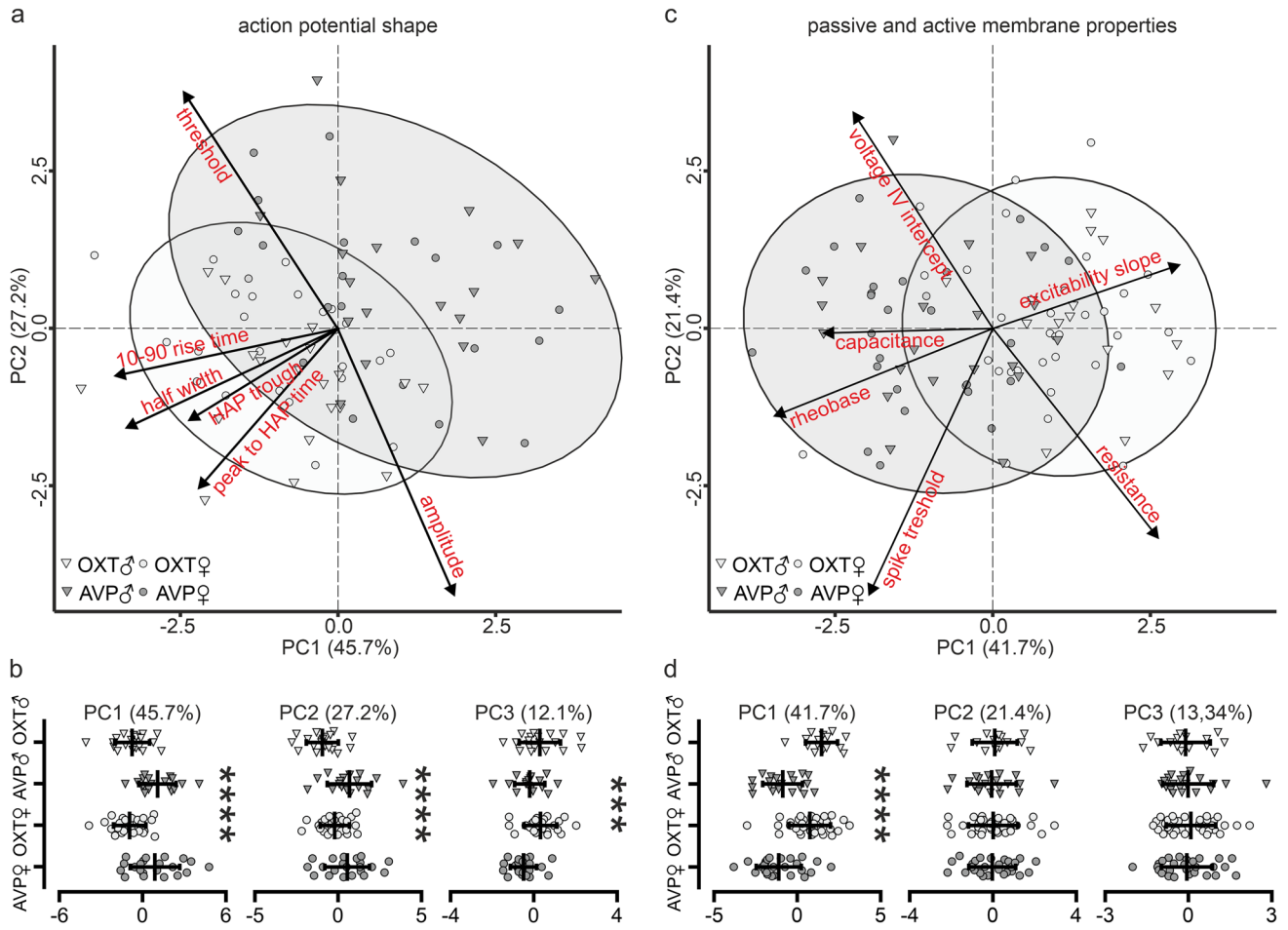

Fig. 5 Principal component analysis of PVN magnocellular neurosecretory cell electrophysiological properties. **a**, **c** Scatter plots of the first two principal components of **a** action potential parameters and **c** membrane properties. Ellipses encompass 90% of OXT (light grey) and AVP (dark grey) MNCs. Arrows represent the loadings of all parameters used in PCA; their length was quadrupled for clarity. **b**, **d** Strip charts showing the principal components for the **b** action potential parameters and **d** membrane properties of four MNC groups: male putative oxytocin (OXT♂), male putative vasopressin (AVP♂), female putative oxytocin (OXT♀), and female putative vasopressin (AVP♀) neurons. Lines and whiskers represent means and SDs. Symbols indicate statistical significance in two-way ANOVA: differences between putative OXT and AVP MNCs are marked as *** ($p < 0.001$) and **** ($p < 0.0001$)

Eventually, differences in PVN OXT MNC innervation and activity of PVN input structures may account for the plasma OXT level, independent of the cell number. Finally, MNCs clustered in the SON and accessory hypothalamic nuclei, which were not subjects of the present study, also contribute to the final release of these peptides and may determine sex differences in their plasma levels.

We also showed a higher number of PVN AVP-ir neurons in male Sprague-Dawley rats than in female rats; however, in other rat strains (Wistar) and in California mice, no sex differences in the number of AVP PVN neurons were observed (Steinman et al. 2015; Dumais and Veenema 2016), which again point to species differences and/or different cell counting approaches. Interestingly, a higher number of AVP neurons in men than in women was shown, which matches the plasma AVP concentrations in both sexes (Share et al. 1988). Importantly, sexual dimorphism in the AVP-ir cell number was described in several other brain regions. The bed nucleus of the stria terminalis (BNST) and medial amygdala (MeA) AVP neurons are also more numerous in males than females in both rodents and non-mammalian vertebrate species (in which differences in vasotocin neurons and AVP homologues were reported; reviewed in De Vries and Panzica 2006). More AVP neurons in the PVN and other brain regions may contribute to the reported higher AVP plasma levels in males than in females as well as to the specific role of this nanopeptide in the regulation of male aggression and social status (Terranova et al. 2016).

The PVN consists of heterogeneous neuronal subpopulations, which are largely segregated into specific subnuclei (magnocellular neurons in the PaLM and PaMM regions and parvocellular neurons in the PaV, PaMP, and PaDC regions)

that differ in their projection patterns; MNCs in the PaLM and PaMM innervate not only the posterior pituitary but also forebrain areas, including the hippocampus and amygdala, whereas parvocellular neurons in the PaMP project mainly to the median eminence, and neurons in the PaV and PaDC constitute descending projections to the spinal cord and several brain stem regions (Armstrong 2015). Importantly, sex differences in the numbers of both OXT and AVP PVN neurons were found to arise mainly from the PaMM part of the PVN, which lies in the most anterior magnocellular subdivision of the nucleus; therefore, we assigned the observed differences to OXT and AVP MNCs. Interestingly, the PaMM, unlike the PaLM or SON, has been shown to be heavily innervated by ACTH-ir fibres (Knigge and Joseph 1982; Piekut 2003) (studies in males only). This phenomenon constitutes the anatomical substrate for the possible involvement of PaMM MNCs in the neuronal circuits controlling learning and arousal-related processes, as these roles were suggested for ACTH-synthesizing neurons in different brain areas (Pranzatelli 1994).

The presented neuroanatomical data indicating sex differences in the numbers of PVN OXT- and AVP-ir neurons constitute an important addition to the understanding of the mechanisms underlying gender diversities in OXT and AVP actions, although sex-specific innervation and receptor expression patterns as well as MNC sensitivity to distinct stimuli are undeniably important factors shaping these actions.

OXT and AVP MNC action potentials

The present study offers an in-depth analysis of PVN MNC electrophysiological features of both sexes. Since the vast majority of available data concerning the electrophysiological properties of MNCs comes from the SON (Brown et al. 2013) and PVN and SON MNCs are assumed to possess similar properties (Tasker and Dudek 1991), in the following discussion, we mainly refer to studies performed on SON MNCs (nonetheless, no study thus far has directly compared PVN and SON MNC electrophysiological properties). First, we will discuss differences between OXT and AVP MNC electrophysiology, whereas sex differences will be addressed later.

The AP shape differs strikingly among neuronal cells (Bean 2007) and influences hormone release by shaping the firing pattern. Here, we examined the AP components of PVN MNCs and revealed several differences as well as similarities between OXT and AVP neurons. In intracellular recordings with sharp electrodes, SON OXT MNCs have been shown to have a smaller AP amplitude than AVP cells in female rats but not in male rats (Armstrong et al. 1994; Stern and Armstrong 1996), whereas our whole-cell patch-clamp recordings did not reveal differences in AP amplitude between male and female MNCs. These discrepancies can largely be attributed to the different recording techniques, because the AP amplitude is largely affected by the capacitance of the recording electrode. We showed herein that the AP threshold in OXT MNCs did not differ from that in AVP MNCs when elicited with a brief current pulse, but was significantly lower when APs were elicited with current ramps. Conversely, previous intracellular recordings have shown that in the SON, OXT neurons have a more depolarized AP threshold than AVP MNCs (Stern and Armstrong, 1996, study in females) and are positively correlated with the baseline membrane potential in only OXT cells (Scroggs et al. 2013, study in females). Our current data clearly show the dependence of the MNC threshold potential on the AP elicitation method, which may underlie the described discrepancies. Additionally, the AP threshold in OXT MNCs was proposed to be more depolarized due to the SOR underlined by non-inactivating K^+ conductance (Stern and Armstrong 1997; Armstrong et al. 2019). However, the SOR requires depolarization to approximately − 60 mV to become active and thus had little influence on OXT MNC properties in the current study, as all neurons were set to − 75 mV baseline for testing. Therefore, the possible influence of the SOR on OXT MNC properties will not be further discussed.

In our study, AVP MNCs exhibited narrower APs with faster rise times than OXT MNCs. The shorter rise time of AVP MNC APs is in line with the previous findings, demonstrating that SON AVP neurons had faster rising APs than OXT neurons, underlined by a greater transient voltage-dependent Na^+ current density (Scroggs et al. 2013).

Traditionally, the terms HAP and afterhyperpolarization (AHP) have fixed specific meanings in MNC electrophysiology. HAP (also referred to as fast afterhyperpolarization—fAHP) follows single APs, whereas AHP is induced by AP trains (Oliet and Bourque 1992; Armstrong et al. 1994). HAPs and AHPs differ in ionic mechanisms and pharmacology (Roper et al. 2003; Armstrong et al. 2019). Here, we showed that when an AP was evoked with a single depolarizing pulse from − 75 mV, the following HAP had faster kinetics and reached more hyperpolarized potentials in AVP MNCs than in OXT MNCs. Among the currents underlying MNC HAPs are the A-current carried by A-type channels and the IK current flux through delayed rectifier channels that shape the first faster component of HAP, which is then sustained by activation of the Ic current carried by BK channels (Bourque 1988; Roper et al. 2003; Komendantov et al. 2007). In our stimulation protocol, the time from the AP peak to the HAP trough was more than ten times shorter in AVP MNCs than in OXT MNCs. The narrower spikes and faster repolarization kinetics of AVP MNCs compared to those of OXT MNCs can be attributed to the greater A-current amplitude and slow inactivating component reported for AVP MNCs as well as to the higher

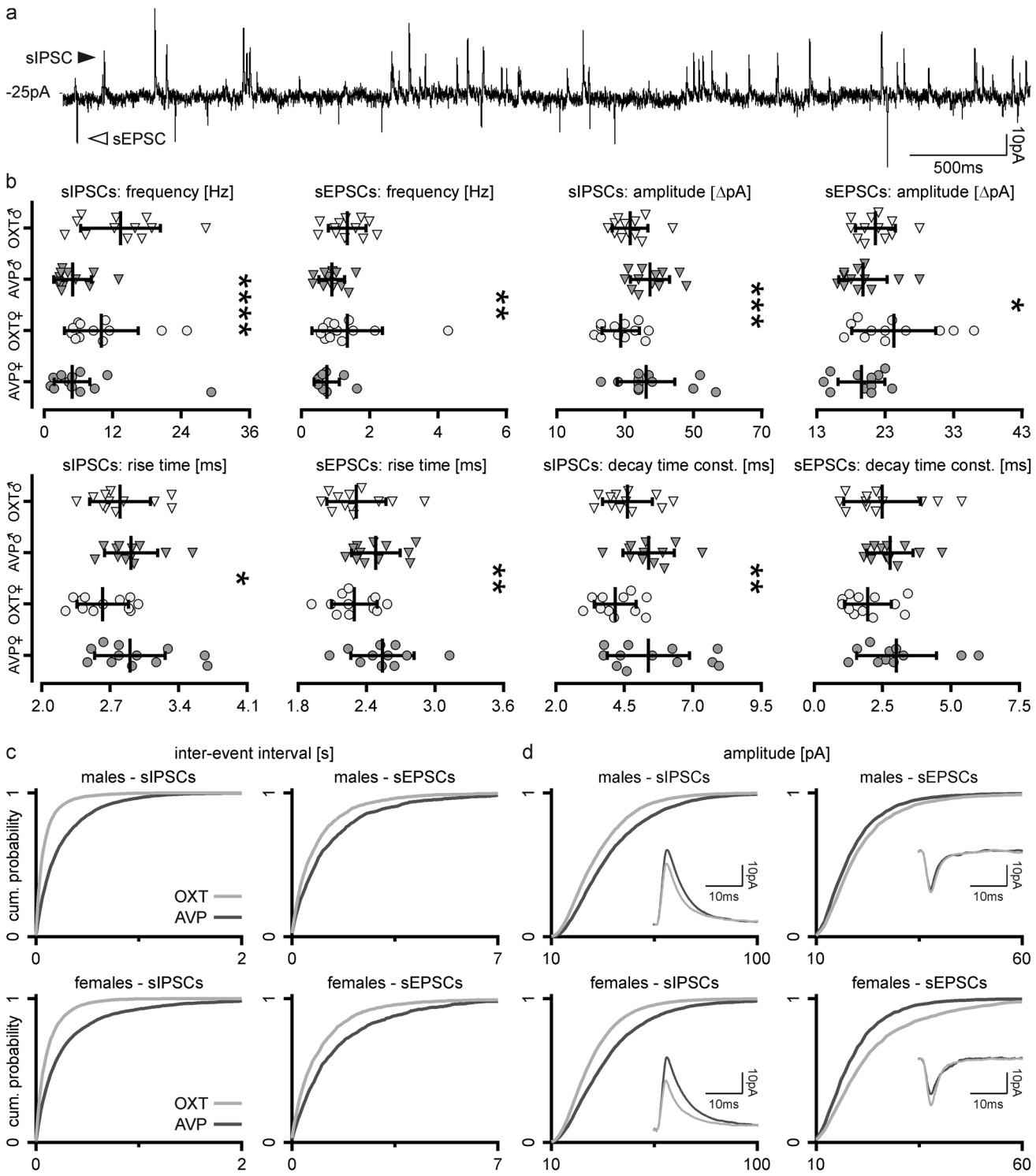

expression of Kv3.1b channel subunits, contributing to IK generation (Fisher et al. 1998; Shevchenko et al. 2004). As 4-aminopyridine, a blocker of the A-current, has been shown to increase the AP duration and influence HAPs in MNCs (Bourque 1988), the striking difference observed in the time course of HAPs may have resulted largely from A-current differences between OXT and AVP MNCs. Alternatively, we propose that in OXT MNCs, in which the A-current is weaker, the characteristic slower HAP kinetics are mainly Ic-current-dependent. Additionally, as MNC HAPs are generated largely by Ca^{2+}-dependent potassium currents (Bourque et al. 1985; Bourque 1988; Dopico et al. 1999; Roper et al. 2003), the higher density of whole-cell Ca^{2+} current in AVP vs. OXT MNCs (Teruyama and Armstrong 2005) may

◂**Fig. 6** Spontaneous synaptic inputs to PVN magnocellular neurosecretory cells. **a** Exemplary trace of MNC spontaneous synaptic events recorded in voltage clamp at a −50 mV holding potential (top). Inhibitory postsynaptic currents (sIPSCs, black arrowhead) are visible as upward deflections, and excitatory postsynaptic currents (sEPSCs, white arrowhead) are visible as downward deflections. Note the prevailing inhibitory synaptic activity. The analysed parameters were obtained from single (frequency, amplitude, and rise time) or mean events (decay time constant). **b** Strip charts showing the spontaneous postsynaptic current parameters of four MNC groups: male putative oxytocin (OXT♂), male putative vasopressin (AVP♂), female putative oxytocin (OXT♀), and female putative vasopressin (AVP♀) neurons. Lines and whiskers represent means and SDs. Symbols indicate statistical significance in two-way ANOVA: differences between putative OXT and AVP MNCs are marked as * ($p<0.05$), ** ($p<0.01$), *** ($p<0.001$), and **** ($p<0.0001$). **c** Cumulative frequency distribution histograms of the sIPSC (bin: 10 ms) and sEPSC (bin: 50 ms) mean interevent intervals. Individual sexes were plotted separately for clarity. **d** Cumulative frequency distribution histograms of sIPSC and sEPSC mean amplitudes (bin: 1 pA). Individual sexes were plotted separately for clarity. Insets show representative averaged synaptic currents

shape their distinct HAPs. However, the possible involvement of other currents and cell type-specific conductances generating HAPs remain to be experimentally verified.

Interestingly, as summarized in the introduction of this paper, several attempts have been made to electrophysiologically distinguish OXT from AVP MNCs, but have failed to provide the final discriminating criteria (da Silva et al. 2015). Several reasons may explain why the highly discriminative time course of HAPs described herein has been overlooked. First, the majority of studies on MNC electrophysiology to date focus on post-burst AHPs and not HAPs (Oliet and Bourque 1992; Armstrong et al. 1994; Armstrong 1995). Second, the recording technique (whole cell vs. sharp intracellular) may obscure the electrophysiological properties of MNCs, as was shown for the SOR in OXT MNCs (da Silva et al. 2015; Armstrong et al. 2019). Third and most likely, the observed difference in MNC HAPs may depend heavily on voltage. Here, we induced APs from a hyperpolarized membrane state (−75 mV), whereas previous studies considered spikes elicited from potentials just below the threshold (Stern and Armstrong 1996; Teruyama and Armstrong 2002). Notably, slower HAPs of OXT MNCs being voltage-independent would have resulted in a lower maximal frequency and lower excitability of OXT vs. AVP MNCs, and we showed exactly the opposite in the current study.

Passive and active electrical properties of OXT and AVP MNCs

Passive electrical properties, such as membrane resistance, time constants and capacitance, mediate the effect of synaptic input in modulating membrane potential and influence neuronal excitability. The lower membrane resistance accompanied by the higher membrane capacitance of AVP MNCs compared to those of OXT MNCs observed in our study is in line with morphometric data demonstrating larger AVP-ir vs. OXA-ir neurons in the SON and PVN across several species, including humans (Kawata and Sano 1982; Schimchowitsch et al. 1989; Lazcano et al. 1990; Ishunina and Swaab 1999). Similar differences in membrane resistance were observed in female SONs in one patch-clamp study (Li et al. 2007), where membrane resistance was assessed based on hyperpolarizing current stimulation, similar to the present study. Another study, in which voltage clamp stimulation from a more depolarized potential (−60 mV vs. −75 mV in the current study) was utilized to calculate the input resistance, reported no differences, pointing to distinct stimulation protocols as the cause of the observed discrepancy (Stern et al. 1999). Described differences in passive membrane properties may underlie the observed excitability of OXT MNCs being higher than that of AVP MNCs (reflected by lower rheobase, higher maximal spiking frequency, and stronger input–output relationship). Additionally, several other factors may have contributed to the reported lower excitability of AVP MNCs. The more profound A-current in AVP vs. OXT MNCs not only delays the occurrence of the AP, but also causes more robust spike broadening in AP trains (Hlubek and Cobbett 2000), resulting in a lower maximal frequency. Finally, AVP MNCs display a greater spiking frequency adaptation than OXT MNCs (Stern and Armstrong 1996; Teruyama and Armstrong 2002), which may further shape their distinct excitability.

Previous studies on female rat SONs showed that AVP but not OXT MNCs display inward rectification in response to hyperpolarizing voltages steps (Stern and Armstrong 1995). Studies in guinea pigs by Erickson et al. attributed this rectification to the H-current being present more frequently in AVP neurons than in OXT neurons and proposed its role in phasic firing generation in AVP MNCs (Erickson et al. 1990, 1993). Here, we demonstrated a more profound voltage sag amplitude in response to strong hyperpolarization in AVP MNCs corresponding to the inward rectification. Moreover, the more prominent voltage sag in AVP MNCs most likely contributed to the little yet significantly more depolarized intercepts calculated for the linear steady-state voltage I–V relationship in AVP vs. OXT MNCs (−80 mV vs −84 mV). As previously reported for hyperpolarized MNCs in the SON, both OXT and AVP neurons displayed a similar linear steady-state voltage I–V relationship (Hoffman et al. 1991; Armstrong et al. 1994; Stern and Armstrong 1995). Similarly, the steady-state current I–V relationship measured herein in voltage clamp showed the outward rectification characteristic of MNCs (Cobbett et al. 1989; Li and Ferguson 1996; Hlubek and Cobbett 1997).

OXT and AVP MNC synaptic input

Synaptic input relays neuronal communication and, together with intrinsic membrane properties, shapes neuronal activity. Spontaneous postsynaptic activity recorded from PVN MNCs in the present study was dominated by inhibitory inputs, similar to MNCs in the SON (Li et al. 2007). This observation is in line with the local origin of GABAergic inputs to the PVN, which may be well preserved in slice preparation (Tasker and Dudek 1993; Boudaba et al. 1996). Moreover, for the first time, we showed that almost all examined parameters describing spontaneous synaptic inputs are different between OXT and AVP MNCs, with OXT MNCs having a higher frequency, lower amplitude, and faster kinetics of sIPSCs as well as a higher frequency, amplitude, and faster kinetics of sEPSCs when compared to AVP MNCs. Interestingly, several analogous differences were reported previously for some mIPSCs and AMPA-mediated mEPSC parameters in the SON, pointing to similarities in synaptic input between MNCs localized in different hypothalamic nuclei (Stern et al. 1999; Li et al. 2007). Distinct innervation patterns as well as differences in the ion-channel properties have been identified and surely contribute to this phenomenon (Stern et al. 1999; Armstrong 2015). Eventually, recent findings that GABAergic neurotransmission is excitatory specifically in AVP MNCs (in a physiological state-dependent manner) should be considered concerning the final outcome of cell type-specific synaptic input on MNC activity (Haam et al. 2012; Morton et al. 2014; Choe et al. 2016).

Sex differences in OXT and AVP MNC electrophysiology

Despite decades of research on the organizational and activational effects of gonadal hormones on brain development and functioning in adulthood, detailed knowledge of the sex-specific properties of neurons is still missing. This deficiency mainly stems from the underrepresentation of female subjects in electrophysiological and anatomical studies and the fact that many studies that are conducted in both sexes fail to analyse results by sex (Beery and Zucker 2011). Nonetheless, growing evidence points to sex-specific properties of neurons contributing to sex differences in brain functioning and behaviour (Abi-Gerges et al. 2004; Cao et al. 2018).

The hypothalamic PVN is a place wherein many neurotransmitters with sex-specific roles are synthesized, and PVN MNCs are among the most comprehensively studied peptidergic neurons in the mammalian brain. However, to the best of our knowledge, there has been no systematic comparison of their electric properties addressing possible sex differences. Only two studies, both from more than 2 decades ago, directly compared the electrophysiological properties of male and female MNCs. Erickson et al. (1993), using intracellular recordings, showed that only the membrane time constant in guinea pig SON MNCs was different in males and females, whereas intracellular recordings in hypothalamic organotypic cultures by Jourdain et al. (1996) reported no sex differences in the basal electrical properties of MNCs. However, due to differences in the recording techniques and tissue preparations, these data cannot be directly compared to the current report.

Our analysis of PVN MNC features revealed that the majority of their intrinsic electrical properties are similar between male and female rats. Nevertheless, we identified the following sex differences in MNC electrophysiology: higher input resistance in male vs. female MNCs and slower HAP kinetics in male vs. female OXT MNCs. However, higher input resistance in males was not accompanied by different membrane capacitance, excluding possible sex differences in the size of MNCs in rats, in contrast to reports in humans (Ishunina and Swaab 1999). Interestingly, these differences in input resistance and HAP kinetics did not result in sex-specific changes in excitability, inferring their voltage dependence. In a study examining the phasic properties of putative OXT SON neurons from male and lactating female rats, Wang and Hatton (2005) showed that in males, APs during bursts have a faster rise time and a tendency towards narrower widths; such differences, according to our data, are not present when properties of single AP are compared between virgin female and male OXT MNCs. Several other MNC electrical properties have been shown to be altered by different, specialized physiological states, such as pregnancy and lactation, indicating their sex dependence (Stern and Armstrong 1996; Teruyama and Armstrong 2002, 2005).

Considering sex differences in HAP kinetics, we showed that the time from the AP peak to the HAP trough is significantly longer in male OXT MNCs than in female OXT MNCs. Because the HAPs of OXT MNCs lack the fast overshoot characteristic of AVP MNCs, we suggest herein that slower kinetics in OXT neurons are dependent on the Ic carried by BK channels (Roper et al. 2003). The lack of sex differences in the AP rise time and half width further confirms that the observed variations in male and female OXT MNCs arise mainly from the slow component of HAP and, therefore, may stem from sex-specific expression of BK channels. Notably, such sex differences in BK channels have been reported in the rat amygdala (Ohno et al. 2009). Nevertheless, the source of observed sex differences in PVN MNCs remains to be thoroughly studied and identified.

Conclusions

Our results show partially distinct electrophysiological profiles of OXT and AVP MNCs, with action potential shapes being unique to each subpopulation. These cell type-specific

differences are accompanied by the overall similarity of male and female MNC electrophysiology. Nevertheless, we identified individual electrophysiological parameters varying between male and female PVN MNCs. Moreover, our anatomical studies further strengthen the role of OXT and AVP systems anatomy in sex-specific behaviours (Dumais and Veenema 2016).

Finally, since distinctive roles of OXT and AVP in females and males most likely arise from a combination of diverse intrinsic MNC properties and extrinsic factors, both aspects should be considered when examining the roles of these nanopeptides in different processes. This notion is of particular importance for studies aimed at unravelling neuronal mechanisms of sex differences in the prevalence and course of various psychiatric disorders, such as autism (Xu et al. 2013; LoParo and Waldman 2015), schizophrenia (Jobst et al. 2014; Aydın et al. 2018), and depression (Yuen et al. 2014; Massey et al. 2016), in which the involvement of AVP and OXT has been implicated.

Author contributions AK and AB conceived the project; AK, AB, PS, AG, AS, ZS, TB, GH, and ZR contributed to the data acquisition and interpretation of the results; AK performed, analysed, and interpreted the ex vivo electrophysiology data; PS and AS performed and analysed the ex vivo electrophysiology data; AK and AG performed the immunostaining and analysed and interpreted the resultant microscopy data; TB created the analysis tools; and AK and AB wrote the article. All authors provided comments and corrections and approved the final version of the manuscript.

Funding This study was funded by research grants from the Ministry of Science and Higher Education (MSHE Poland 0020/DIA/2014/43 to A.K.), the National Science Centre (NSC Poland, DEC-2012/05/D/NZ4/02984 to A.B.), and the Institute of Zoology and Biomedical Research of the Jagiellonian University in Krakow (DS/MND/WBiNoZ/IZ/20/2016, K/DSC/003960 and DS/MND/WBiNoZ/IZ/16/2017, K/DSC/004650). A.K. obtained founding from the National Science Centre's Ph.D. scholarship programme ETIUDA V (NSC Poland, UMO-2017/24/T/NZ4/00225).

Compliance with ethical standards

Conflicts of interest The authors have no conflicts of interest to declare.

Human and animal participants right statement This article does not contain any studies involving human participants that were performed by any of the authors.

References

Abi-Gerges N, Small BG, Lawrence CL et al (2004) Evidence for gender differences in electrophysiological properties of canine Purkinje fibres. Br J Pharmacol 142:1255–1264. https://doi.org/10.1038/sj.bjp.0705880

Armstrong WE (1995) Morphological and electrophysiological classification of hypothalamic supraoptic neurons. Prog Neurobiol 47:291–339. https://doi.org/10.1016/0301-0082(95)80005-S

Armstrong WE (2015) Chapter 14. Hypothalamic supraoptic and paraventricular nuclei. In: Paxinos G (ed) The rat nervous system, 4th edn. Academic Press, Cambridge, pp 295–314

Armstrong WE, Tasker JG (eds) (2014) Neurophysiology of neuroendocrine neurons. Wiley, Chichester

Armstrong WE, Smith BN, Tian M (1994) Electrophysiological characteristics of immunochemically identified rat oxytocin and vasopressin neurones in vitro. J Physiol 475:115–128. https://doi.org/10.1113/jphysiol.1994.sp020053

Armstrong WE, Foehring RC, Kirchner MK, Sladek CD (2019) Electrophysiological properties of identified oxytocin and vasopressin neurones. J Neuroendocrinol. https://doi.org/10.1111/jne.12666

Aydın O, Lysaker PH, Balıkçı K et al (2018) Associations of oxytocin and vasopressin plasma levels with neurocognitive, social cognitive and meta cognitive function in schizophrenia. Psychiatry Res 270:1010–1016. https://doi.org/10.1016/j.psychres.2018.03.048

Bangasser DA, Wicks B (2017) Sex-specific mechanisms for responding to stress. J Neurosci Res 95:75–82. https://doi.org/10.1002/jnr.23812

Baribeau DA, Anagnostou E (2015) Oxytocin and vasopressin: linking pituitary neuropeptides and their receptors to social neurocircuits. Front Neurosci 9:335. https://doi.org/10.3389/fnins.2015.00335

Barna J, Dimén D, Puska G et al (2019) Complement component 1q subcomponent binding protein in the brain of the rat. Sci Rep 9:4597. https://doi.org/10.1038/s41598-019-40788-z

Bean BP (2007) The action potential in mammalian central neurons. Nat Rev Neurosci 8:451–465. https://doi.org/10.1038/nrn2148

Beery AK, Zucker I (2011) Sex bias in neuroscience and biomedical research. Neurosci Biobehav Rev 35:565–572. https://doi.org/10.1016/j.neubiorev.2010.07.002

Bendesky A, Kwon Y-M, Lassance J-M et al (2017) The genetic basis of parental care evolution in monogamous mice. Nature 544:434–439. https://doi.org/10.1038/nature22074

Bosch OJ, Neumann ID (2012) Both oxytocin and vasopressin are mediators of maternal care and aggression in rodents: from central release to sites of action. Horm Behav 61:293–303. https://doi.org/10.1016/j.yhbeh.2011.11.002

Boudaba C, Szabó K, Tasker JG (1996) Physiological mapping of local inhibitory inputs to the hypothalamic paraventricular nucleus. J Neurosci 16:7151–7160. https://doi.org/10.1523/JNEUROSCI.16-22-07151.1996

Bourque CW (1988) Transient calcium-dependent potassium current in magnocellular neurosecretory cells of the rat supraoptic nucleus. J Physiol 397:331–347. https://doi.org/10.1113/jphysiol.1988.sp017004

Bourque CW, Randle JC, Renaud LP (1985) Calcium-dependent potassium conductance in rat supraoptic nucleus neurosecretory neurons. J Neurophysiol 54:1375–1382. https://doi.org/10.1152/jn.1985.54.6.1375

Bredewold R, Veenema AH (2018) Sex differences in the regulation of social and anxiety-related behaviors: insights from vasopressin and oxytocin brain systems. Curr Opin Neurobiol 49:132–140. https://doi.org/10.1016/j.conb.2018.02.011

Brown CH, Bains JS, Ludwig M, Stern JE (2013) Physiological regulation of magnocellular neurosecretory cell activity: integration of intrinsic, local and afferent mechanisms. J Neuroendocrinol 25:678–710. https://doi.org/10.1111/jne.12051

Caldwell HK (2017) Oxytocin and vasopressin: powerful regulators of social behavior. Neuroscientist 23:517–528. https://doi.org/10.1177/1073858417708284

Cao J, Willett JA, Dorris DM, Meitzen J (2018) Sex differences in medium spiny neuron excitability and glutamatergic synaptic

input: heterogeneity across striatal regions and evidence for estradiol-dependent sexual differentiation. Front Endocrinol (Lausanne) 9:173. https://doi.org/10.3389/fendo.2018.00173

Choe KY, Trudel E, Bourque CW (2016) Effects of salt loading on the regulation of rat hypothalamic magnocellular neurosecretory cells by ionotropic GABA and glycine receptors. J Neuroendocrinol. https://doi.org/10.1111/jne.12372

Cobbett P, Legendre P, Mason WT (1989) Characterization of three types of potassium current in cultured neurones of rat supraoptic nucleus area. J Physiol 410:443–462. https://doi.org/10.1113/jphysiol.1989.sp017543

da Silva MP, Merino RM, Mecawi AS et al (2015) In vitro differentiation between oxytocin- and vasopressin-secreting magnocellular neurons requires more than one experimental criterion. Mol Cell Endocrinol 400:102–111. https://doi.org/10.1016/j.mce.2014.11.004

de Vries GJ (2008) Sex differences in vasopressin and oxytocin innervation of the brain. Prog Brain Res 170:17–27. https://doi.org/10.1016/S0079-6123(08)00402-0

De Vries GJ, Panzica GC (2006) Sexual differentiation of central vasopressin and vasotocin systems in vertebrates: different mechanisms, similar endpoints. Neuroscience 138:947–955. https://doi.org/10.1016/j.neuroscience.2005.07.050

Dopico AM, Widmer H, Wang G et al (1999) Rat supraoptic magnocellular neurones show distinct large conductance, Ca^{2+}-activated K^+ channel subtypes in cell bodies versus nerve endings. J Physiol 519(Pt 1):101–114. https://doi.org/10.1111/j.1469-7793.1999.0101o.x

Dumais KM, Veenema AH (2016) Vasopressin and oxytocin receptor systems in the brain: sex differences and sex-specific regulation of social behavior. Front Neuroendocrinol 40:1–23. https://doi.org/10.1016/j.yfrne.2015.04.003

Eliava M, Melchior M, Knobloch-Bollmann HS et al (2016) A new population of parvocellular oxytocin neurons controlling magnocellular neuron activity and inflammatory pain processing. Neuron 89:1291–1304. https://doi.org/10.1016/j.neuron.2016.01.041

Erickson KR, Ronnekleiv OK, Kelly MJ (1990) Inward rectification (I) in immunocytochemically-ldentified vasopressin and oxytocin neurons of guinea-pig supraoptic nucleus. J Neuroendocrinol 2:261–265. https://doi.org/10.1111/j.1365-2826.1990.tb00402.x

Erickson KR, Ronnekleiv OK, Kelly MJ (1993) Electrophysiology of guinea-pig supraoptic neurones: role of a hyperpolarization-activated cation current in phasic firing. J Physiol 460:407–425. https://doi.org/10.1113/jphysiol.1993.sp019478

Fisher TE, Voisin DL, Bourque CW (1998) Density of transient K^+ current influences excitability in acutely isolated vasopressin and oxytocin neurones of rat hypothalamus. J Physiol 511(Pt 2):423–432. https://doi.org/10.1111/j.1469-7793.1998.423bh.x

Haam J, Popescu IR, Morton LA et al (2012) GABA is excitatory in adult vasopressinergic neuroendocrine cells. J Neurosci 32:572–582. https://doi.org/10.1523/JNEUROSCI.3826-11.2012

Hatton GI, Wang Y-F (2008) Neural mechanisms underlying the milk ejection burst and reflex. Prog Brain Res 170:155–166. https://doi.org/10.1016/S0079-6123(08)00414-7

Hazell GGJ, Hindmarch CC, Pope GR et al (2012) G protein-coupled receptors in the hypothalamic paraventricular and supraoptic nuclei–serpentine gateways to neuroendocrine homeostasis. Front Neuroendocrinol 33:45–66. https://doi.org/10.1016/j.yfrne.2011.07.002

Hernández VS, Vázquez-Juárez E, Márquez MM et al (2015) Extra-neurohypophyseal axonal projections from individual vasopressin-containing magnocellular neurons in rat hypothalamus. Front Neuroanat 9:130. https://doi.org/10.3389/fnana.2015.00130

Hirasawa M, Mouginot D, Kozoriz MG et al (2003) Vasopressin differentially modulates non-NMDA receptors in vasopressin and oxytocin neurons in the supraoptic nucleus. J Neurosci 23:4270–4277. https://doi.org/10.1523/JNEUROSCI.23-10-04270.2003

Hlubek MD, Cobbett P (1997) Outward potassium currents of supraoptic magnocellular neurosecretory cells isolated from the adult guinea-pig. J Physiol 502(Pt 1):61–74. https://doi.org/10.1111/j.1469-7793.1997.061bl.x

Hlubek MD, Cobbett P (2000) Differential effects of K(+) channel blockers on frequency-dependent action potential broadening in supraoptic neurons. Brain Res Bull 53:203–209. https://doi.org/10.1016/S0361-9230(00)00335-X

Hoffman NW, Tasker JG, Dudek FE (1991) Immunohistochemical differentiation of electrophysiologically defined neuronal populations in the region of the rat hypothalamic paraventricular nucleus. J Comp Neurol 307:405–416. https://doi.org/10.1002/cne.903070306

Horn JP, Swanson LW (2013) Chapter 47: the autonomic motor system and the hypothalamus. In: Kandel EK, Schwartz JH, Jessell TM et al (eds) Principles of neural science, 5th edn. McGraw-Hill Medical, New York, pp 1056–1078

Hou-Yu A, Lamme AT, Zimmerman EA, Silverman AJ (1986) Comparative distribution of vasopressin and oxytocin neurons in the rat brain using a double-label procedure. Neuroendocrinology 44:235–246. https://doi.org/10.1159/000124651

Ishunina TA, Swaab DF (1999) Vasopressin and oxytocin neurons of the human supraoptic and paraventricular nucleus: size changes in relation to age and sex. J Clin Endocrinol Metab 84:4637–4644. https://doi.org/10.1210/jcem.84.12.6187

Jobst A, Dehning S, Ruf S et al (2014) Oxytocin and vasopressin levels are decreased in the plasma of male schizophrenia patients. Acta Neuropsychiatr 26:347–355. https://doi.org/10.1017/neu.2014.20

Jourdain P, Poulain DA, Theodosis DT, Israel JM (1996) Electrical properties of oxytocin neurons in organotypic cultures from postnatal rat hypothalamus. J Neurophysiol 76:2772–2785. https://doi.org/10.1152/jn.1996.76.4.2772

Jurek B, Neumann ID (2018) The oxytocin receptor: from intracellular signaling to behavior. Physiol Rev 98:1805–1908. https://doi.org/10.1152/physrev.00031.2017

Kania A, Gugula A, Grabowiecka A et al (2017) Inhibition of oxytocin and vasopressin neuron activity in rat hypothalamic paraventricular nucleus by relaxin-3-RXFP3 signalling. J Physiol 595:3425–3447. https://doi.org/10.1113/JP273787

Karim MA, Sloper JC (1980) Histogenesis of the supraoptic and paraventricular neurosecretory cells of the mouse hypothalamus. J Anat 130:341–347

Kastman HE, Blasiak A, Walker L et al (2016) Nucleus incertus Orexin2 receptors mediate alcohol seeking in rats. Neuropharmacology 110:82–91. https://doi.org/10.1016/j.neuropharm.2016.07.006

Kawata M, Sano Y (1982) Immunohistochemical identification of the oxytocin and vasopressin neurons in the hypothalamus of the monkey (*Macaca fuscata*). Anat Embryol (Berl) 165:151–167. https://doi.org/10.1007/BF00305474

Knigge KM, Joseph SA (1982) Relationship of the central ACTH-immunoreactive opiocortin system to the supraoptic and paraventricular nuclei of the hypothalamus of the rat. Brain Res 239:655–658. https://doi.org/10.1016/0006-8993(82)90545-5

Knobloch HS, Grinevich V (2014) Evolution of oxytocin pathways in the brain of vertebrates. Front Behav Neurosci 8:31. https://doi.org/10.3389/fnbeh.2014.00031

Knobloch HS, Charlet A, Hoffmann LC et al (2012) Evoked axonal oxytocin release in the central amygdala attenuates fear response. Neuron 73:553–566. https://doi.org/10.1016/j.neuron.2011.11.030

Komendantov AO, Trayanova NA, Tasker JG (2007) Somato-dendritic mechanisms underlying the electrophysiological properties of hypothalamic magnocellular neuroendocrine cells: a

multicompartmental model study. J Comput Neurosci 23:143–168. https://doi.org/10.1007/s10827-007-0024-z
Koshimizu T, Nakamura K, Egashira N et al (2012) Vasopressin V1a and V1b receptors: from molecules to physiological systems. Physiol Rev 92:1813–1864. https://doi.org/10.1152/physrev.00035.2011
Kramer KM, Cushing BS, Carter CS et al (2004) Sex and species differences in plasma oxytocin using an enzyme immunoassay. Can J Zool 82:1194–1200. https://doi.org/10.1139/z04-098
Lazcano MA, Bentura ML, Toledano A (1990) Morphometric study on the development of magnocellular neurons of the supraoptic nucleus utilising immunohistochemical methods. J Anat 168:1–11
Leng G, Pineda R, Sabatier N, Ludwig M (2015) 60 years of neuroendocrinology: the posterior pituitary, from Geoffrey Harris to our present understanding. J Endocrinol 226:T173–T185. https://doi.org/10.1530/JOE-15-0087
Li Z, Ferguson AV (1996) Electrophysiological properties of paraventricular magnocellular neurons in rat brain slices: modulation of IA by angiotensin II. Neuroscience 71:133–145. https://doi.org/10.1016/0306-4522(95)00434-3
Li C, Tripathi PK, Armstrong WE (2007) Differences in spike train variability in rat vasopressin and oxytocin neurons and their relationship to synaptic activity. J Physiol 581:221–240. https://doi.org/10.1113/jphysiol.2006.123810
LoParo D, Waldman ID (2015) The oxytocin receptor gene (OXTR) is associated with autism spectrum disorder: a meta-analysis. Mol Psychiatry 20:640–646. https://doi.org/10.1038/mp.2014.77
Ludwig M, Leng G (2006) Dendritic peptide release and peptide-dependent behaviours. Nat Rev Neurosci 7:126–136. https://doi.org/10.1038/nrn1845
Ludwig M, Sabatier N, Bull PM et al (2002) Intracellular calcium stores regulate activity-dependent neuropeptide release from dendrites. Nature 418:85–89. https://doi.org/10.1038/nature00822
Luther JA, Tasker JG (2000) Voltage-gated currents distinguish parvocellular from magnocellular neurones in the rat hypothalamic paraventricular nucleus. J Physiol 523(Pt 1):193–209. https://doi.org/10.1111/j.1469-7793.2000.t01-1-00193.x
Massey SH, Backes KA, Schuette SA (2016) Plasma oxytocin concentration and depressive symptoms: a review of current evidence and directions for future research. Depress Anxiety 33:316–322. https://doi.org/10.1002/da.22467
McCutcheon JE, Marinelli M (2009) Age matters. Eur J Neurosci 29:997–1014. https://doi.org/10.1111/j.1460-9568.2009.06648.x
Meyer-Lindenberg A, Domes G, Kirsch P, Heinrichs M (2011) Oxytocin and vasopressin in the human brain: social neuropeptides for translational medicine. Nat Rev Neurosci 12:524–538. https://doi.org/10.1038/nrn3044
Morton LA, Popescu IR, Haam J, Tasker JG (2014) Short-term potentiation of GABAergic synaptic inputs to vasopressin and oxytocin neurones. J Physiol 592:4221–4233. https://doi.org/10.1113/jphysiol.2014.277293
Nephew BC (2012) Behavioral roles of oxytocin and vasopressin. In: Sumiyoshi T (ed) Neuroendocrinology and behavior. InTech, London, pp 49–82
Ohno A, Ohya S, Yamamura H, Imaizumi Y (2009) Gender difference in BK channel expression in amygdala complex of rat brain. Biochem Biophys Res Commun 378:867–871. https://doi.org/10.1016/j.bbrc.2008.12.004
Oliet SH, Bourque CW (1992) Properties of supraoptic magnocellular neurones isolated from the adult rat. J Physiol 455:291–306. https://doi.org/10.1113/jphysiol.1992.sp019302
Paxinos G, Watson C (2007) The rat brain in stereotaxic coordinates, 6th edn. Academic Press, San Diego
Piekut DT (2003) Relationship of ACTH1-39-immunostained fibers and magnocellular neurons in the paraventricular nucleus of rat hypothalamus. Peptides 6:883–890. https://doi.org/10.1016/0196-9781(85)90319-5
Poulain DA, Wakerley JB (1982) Electrophysiology of hypothalamic magnocellular neurones secreting oxytocin and vasopressin. Neuroscience 7:773–808. https://doi.org/10.1016/0306-4522(82)90044-6
Poulain DA, Wakerley JB, Dyball RE (1977) Electrophysiological differentiation of oxytocin- and vasopressin-secreting neurones. Proc R Soc Lond Ser B Biol Sci 196:367–384. https://doi.org/10.1098/rspb.1977.0046
Pranzatelli MR (1994) On the molecular mechanism of adrenocorticotrophic hormone in the CNS: neurotransmitters and receptors. Exp Neurol 125:142–161. https://doi.org/10.1006/exnr.1994.1018
Raggenbass M (2001) Vasopressin- and oxytocin-induced activity in the central nervous system: electrophysiological studies using in vitro systems. Prog Neurobiol 64:307–326. https://doi.org/10.1016/S0301-0082(00)00064-2
R Core Team (2018) R: a language and environment for statistical computing. R Foundation for Statistical Computing, Vienna. http://www.R-project.org/
Renaud LP, Bourque CW (1991) Neurophysiology and neuropharmacology of hypothalamic magnocellular neurons secreting vasopressin and oxytocin. Prog Neurobiol 36:131–169. https://doi.org/10.1016/0301-0082(91)90020-2
Rhodes CH, Morrell JI, Pfaff DW (1981) Immunohistochemical analysis of magnocellular elements in rat hypothalamus: distribution and numbers of cells containing neurophysin, oxytocin, and vasopressin. J Comp Neurol 198:45–64. https://doi.org/10.1002/cne.901980106
Roper P, Callaway J, Shevchenko T et al (2003) AHP's, HAP's and DAP's: how potassium currents regulate the excitability of rat supraoptic neurones. J Comput Neurosci 15:367–389. https://doi.org/10.1023/A:1027424128972
Roy RK, Augustine RA, Brown CH, Schwenke DO (2018) Activation of oxytocin neurons in the paraventricular nucleus drives cardiac sympathetic nerve activation following myocardial infarction in rats. Commun Biol 1:160. https://doi.org/10.1038/s42003-018-0169-5
Schimchowitsch S, Moreau C, Laurent F, Stoeckel M-E (1989) Distribution and morphometric characteristics of oxytocin- and vasopressin-immunoreactive neurons in the rabbit hypothalamus. J Comp Neurol 285:304–324. https://doi.org/10.1002/cne.902850303
Scroggs R, Wang L, Teruyama R, Armstrong WE (2013) Variation in sodium current amplitude between vasopressin and oxytocin hypothalamic supraoptic neurons. J Neurophysiol 109:1017–1024. https://doi.org/10.1152/jn.00812.2012
Share L, Crofton JT, Ouchi Y (1988) Vasopressin: sexual dimorphism in secretion, cardiovascular actions and hypertension. Am J Med Sci 295:314–319. https://doi.org/10.1097/00000441-198804000-00017
Shevchenko T, Teruyama R, Armstrong WE (2004) High-threshold, Kv3-like potassium currents in magnocellular neurosecretory neurons and their role in spike repolarization. J Neurophysiol 92:3043–3055. https://doi.org/10.1152/jn.00431.2004
Silverman AJ, Zimmerman EA (1983) Magnocellular neurosecretory system. Annu Rev Neurosci 6:357–380. https://doi.org/10.1146/annurev.ne.06.030183.002041
Steinman MQ, Laredo SA, Lopez EM et al (2015) Hypothalamic vasopressin systems are more sensitive to the long term effects of social defeat in males versus females. Psychoneuroendocrinology 51:122–134. https://doi.org/10.1016/j.psyneuen.2014.09.009
Stern JE, Armstrong WE (1995) Electrophysiological differences between oxytocin and vasopressin neurones recorded from

female rats in vitro. J Physiol 488(Pt 3):701–708. https://doi.org/10.1113/jphysiol.1995.sp021001

Stern JE, Armstrong WE (1996) Changes in the electrical properties of supraoptic nucleus oxytocin and vasopressin neurons during lactation. J Neurosci 16:4861–4871. https://doi.org/10.1523/jneurosci.16-16-04861.1996

Stern JE, Armstrong WE (1997) Sustained outward rectification of oxytocinergic neurones in the rat supraoptic nucleus: ionic dependence and pharmacology. J Physiol 500(Pt 2):497–508. https://doi.org/10.1113/jphysiol.1997.sp022036

Stern JE, Galarreta M, Foehring RC et al (1999) Differences in the properties of ionotropic glutamate synaptic currents in oxytocin and vasopressin neuroendocrine neurons. J Neurosci 19:3367–3375. https://doi.org/10.1523/JNEUROSCI.19-09-03367.1999

Stoop R (2012) Neuromodulation by oxytocin and vasopressin. Neuron 76:142–159. https://doi.org/10.1016/j.neuron.2012.09.025

Swaab DF, Pool CW, Nijveldt F (1975) Immunofluorescence of vasopressin and oxytocin in the rat hypothalamo-neurohypophyopseal system. J Neural Transm 36:195–215

Swanson LW, Sawchenko PE (1983) Hypothalamic integration: organization of the paraventricular and supraoptic nuclei. Annu Rev Neurosci 6:269–324. https://doi.org/10.1146/annurev.ne.06.030183.001413

Tasker JG, Dudek FE (1991) Electrophysiological properties of neurones in the region of the paraventricular nucleus in slices of rat hypothalamus. J Physiol 434:271–293. https://doi.org/10.1113/jphysiol.1991.sp018469

Tasker JG, Dudek FE (1993) Local inhibitory synaptic inputs to neurones of the paraventricular nucleus in slices of rat hypothalamus. J Physiol 469:179–192. https://doi.org/10.1113/jphysiol.1993.sp019810

Terranova JI, Song Z, Larkin TE et al (2016) Serotonin and arginine-vasopressin mediate sex differences in the regulation of dominance and aggression by the social brain. Proc Natl Acad Sci USA 113:13233–13238. https://doi.org/10.1073/pnas.1610446113

Teruyama R, Armstrong WE (2002) Changes in the active membrane properties of rat supraoptic neurones during pregnancy and lactation. J Neuroendocrinol 14:933–944. https://doi.org/10.1046/j.1365-2826.2002.00844.x

Teruyama R, Armstrong WE (2005) Enhancement of calcium-dependent afterpotentials in oxytocin neurons of the rat supraoptic nucleus during lactation. J Physiol 566:505–518. https://doi.org/10.1113/jphysiol.2005.085985

Vandesande F, Dierickx K (1975) Identification of the vasopressin producing and of the oxytocin producing neurons in the hypothalamic magnocellular neurosecretroy system of the rat. Cell Tissue Res 164:153–162

Veening JG, de Jong TR, Waldinger MD et al (2015) The role of oxytocin in male and female reproductive behavior. Eur J Pharmacol 753:209–228. https://doi.org/10.1016/j.ejphar.2014.07.045

Wakerley JB, Lincoln DW (1973) The milk-ejection reflex of the rat: a 20- to 40-fold acceleration in the firing of paraventricular neurones during oxytocin release. J Endocrinol 57:477–493

Wang Y-F, Hatton GI (2005) Burst firing of oxytocin neurons in male rat hypothalamic slices. Brain Res 1032:36–43. https://doi.org/10.1016/j.brainres.2004.10.046

Windle RJ, Forsling ML (1993) Variations in oxytocin secretion during the 4-day oestrous cycle of the rat. J Endocrinol 136:305–311. https://doi.org/10.1677/joe.0.1360305

Xu X-J, Shou X-J, Li J et al (2013) Mothers of autistic children: lower plasma levels of oxytocin and Arg-vasopressin and a higher level of testosterone. PLoS One. https://doi.org/10.1371/journal.pone.0074849

Yuen KW, Garner JP, Carson DS et al (2014) Plasma oxytocin concentrations are lower in depressed vs. healthy control women and are independent of cortisol. J Psychiatr Res 51:30–36. https://doi.org/10.1016/j.jpsychires.2013.12.012

Zampronio AR, Kuzmiski JB, Florence CM et al (2010) Opposing actions of endothelin-1 on glutamatergic transmission onto vasopressin and oxytocin neurons in the supraoptic nucleus. J Neurosci 30:16855–16863. https://doi.org/10.1523/JNEUROSCI.5079-10.2010

Zhao Z, Wang L, Gao W et al (2017) A central catecholaminergic circuit controls blood glucose levels during stress. Neuron 95:138–152. https://doi.org/10.1016/j.neuron.2017.05.031